Submitted to ApJ

The Universe Was Reionized Twice

Renyue Cen[1]

ABSTRACT

With a top-heavy initial stellar mass function for Population III stars, as recent simulations seem to suggest, we show that Pop III stars can, for the first time, reionize the universe at $z \sim 15-20$ in the standard cold dark matter cosmological model. The physical reason rests in the positive feedback from Pop III star formation, made possible by a high X-ray background, which, in turn, is produced by supernova blast waves of Pop III stars and miniquasars powered by Pop III black holes both emitting a large fraction of the available energy in X-rays at $\sim$ 1keV at $z \sim 15-25$, As a result, the primary coolant, H_2 molecules, can be abundantly produced in minihalos and Pop III star formation activity is able to continue to build up to the required level for reionization.

The first reionization by massive Pop III stars heats up the intergalactic medium to a high temperature, sharply raising the Jeans mass and causing star formation rate to plunge. Hence, in the immediate aftermath, ionized hydrogen recombines on a time scale of 10^8 yr and the universe once again becomes opaque to Lyα and ionizing photons, entering the second dark age. The long period from the first reionization at $z \sim 15-20$ to the second reionization at $z \sim 6$, however, does not lack interesting actions. Two competing forces, Compton cooling by the cosmic microwave background and photoheating by the stars, regulate the Jeans mass and the star formation rate. The mean temperature of the intergalactic medium is maintained at $5 \times 10^3 - 10^4$ K from $z = 15-20$ to $z = 6$. Another pair of competing forces, namely photoionization and recombination, is also at work such that the mean ionization fraction of the intergalactic medium is kept in a rather narrow range $n_{\rm HII}/n_{\rm H} \sim 0.4-1.0$ from $z = 15-20$ to $z = 6$. At $z \sim 6$, the global star formation rate again surpasses the global recombination rate, resulting in the second reionization of the universe. The second reionization is predominantly due to stars formed in halos where atomic line cooling is efficient. There is no abrupt change of the temperature of the intergalactic medium at the completion of the second reionization.

We discuss implications and possible tests for this new reionization picture.

[1]Princeton University Observatory, Princeton University, Princeton, NJ 08544; cen@astro.princeton.edu

Subject headings: cosmology: theory —intergalactic medium —interstellar medium —supernova —reionization

1. Introduction

The conventional view is that the universe becomes reionized at $z = 6 - 10$, when the star formation rate in galaxies with virial temperatures greater than $\sim 10^4$K (where hydrogen atoms are efficient coolants) exceeds the overall recombination rate (e.g., Barkana & Loeb 2001; Madau 2002).

In this paper we present a new scenario. Adopting the standard cold dark matter cosmological model we show that the universe is first reionized at redshift $z = 15 - 20$ by Population III (Pop III) stars in minihalos having virial temperature below 10^4K. In order to enable a sustained ionizing source from minihalos it is necessary to maintain an adequate level of H_2 molecule fraction within their cores, since H_2 molecules are the only available coolant at the low temperature for the primordial gas free of metals. As is well known, H_2 molecules are very fragile and easily destroyed by photons in the Lyman-Werner bands, $11.18 - 13.6$eV, to which the universe is largely transparent. Primeval H_2 molecules have been completely destroyed well before enough ionizing photons are produced to reionize the universe (Gnedin & Ostriker 1997; Haiman, Rees, & Loeb 1997; Tegmark et al. 1997). Therefore, an adequate production rate of H_2 molecules is required to counteract the destruction rate to keep H_2 fraction at a useful level. A sufficiently high X-ray background at high redshift could serve as a requisite catalyst for forming H_2 molecules by deeply penetrating into and generating a sufficient number of free electrons in the cores of minihalos (Haiman, Abel, & Rees 2000; Ricotti, Gnedin, & Shull 2001; Glover & Bland 2002).

We point out that at redshift $z = 15 - 25$ supernova remnants of Pop III stars and miniquasars powered by Pop III black holes are efficient X-ray emitters. The much higher density of the interstellar medium at high redshift results in a much more rapid and earlier cooling phase of the supernova blast waves, emitting a large fraction of the cooling energy in X-ray energy ($\sim$ 1keV). [In contrast, supernova blast waves in the local galaxies are known not to cool efficiently until their temperatures have dropped well below the X-ray regime (e.g., Cox 1972; Chevalier 1974,1982)]. Separately, miniquasars powered by Pop III black holes of mass $\sim 10 - 100\,M_\odot$ emit a large fraction of the radiation in X-rays at ≥ 1 keV. The combined X-ray emission from Pop III supernova remnants and miniquasars is sufficient to enable efficient H_2 formation and cooling in the cores of minihalo galaxies. By $z = 15 - 20$ the global ionizing photon emission rate from Pop III stars in minihalos exceeds the global recombination rate and the universe is completely reionized and heated.

Following the first reionization, star formation in minihalos is quenched, because gas is either heated (by internal or external UV radiation) and driven out of the shallow potential wells of these minihalos (Shapiro, Raga, & Mellema 1997; Barkana & Loeb 1999) or blown away by supernova explosions (Mac Low & Ferrara 1999; Mori, Ferrara & Madau 2002). Meanwhile, the Jeans mass of the intergalactic medium (IGM) jumps up by three orders of magnitude due to photoheating. Although a low level of star formation activities continues in halos more massive than the new, high Jeans mass, it is insufficient to counterbalance the rapid recombination process. The universe recombines to become opaque to Lyα and ionizing photons, again! For Compton cooling is very efficient at $z = 15 - 25$, the intergalactic gas is overcooled to low temperatures (a few thousand K) but stays significantly ionized.

As time progresses, with the combined effect of increasing density fluctuations (and the nonlinear mass scale) with time and continued cooling, star formation rate gradually picks up. But at $z \leq 10$ supernova remnants may no longer be emitting a large fraction of the cooling energy in X-rays, although miniquasars continue to emit largely in X-rays and can continue to generate an adequate amount of free electrons. Regardless, the first reionization has left a sufficient amount of residual free electrons, which can now serve to enhance the formation of H_2 molecules even in the absence of an external high X-ray background; in the cores of minihalos the free electron fraction is significantly larger than 10^{-3}, above what is needed to form an adequate fraction of H_2 molecules (Haiman et al. 2000). The IGM is maintained at an average temperature of $\sim 5 \times 10^3 - 10^4$ K throughout the entire period from $z = 17$ to $z = 6$, balanced between cooling and continuous heating from photoionization. While H_2 formation is possible, such a relatively high temperature of the IGM hence a high Jeans mass dictates that the dominant fraction of the star formation occurs in large halos where atomic line cooling is important. No sufficient number of ionizing photons is formed until at $z \sim 6$, when the universe is completely reionized for the second time, and for all.

The outline of this paper is as follows. We put forth two new sources of X-ray radiation in §2, namely, the Pop III supernova cooling radiation and X-ray emission from miniquasars. In §3 we identify the epoch of the first reionization by Pop III stars, followed by a detailed analysis of the subsequent evolution including the second cosmological recombination and second reionization in §4. We discuss possible implications and significant consequences of this new scenario in §5 and conclude in §6. Throughout a spatially flat cold dark matter cosmological model with $\Omega_M = 0.25$, $\Omega_b = 0.04$, $\Lambda = 0.75$, $H_0 = 72$km/s/Mpc and $\sigma_8 = 0.8$ is adopted (e.g., Bahcall et al. 2002).

2. X-ray Emission From Pop III Supernovae and Miniquasars, and Hydrogen Molecule Formation

The important role that H_2 molecules play in the collapse of gas clouds to form Pop III stars and the initial mass function of Pop III stars have a long history of investigation (Saslaw & Zipoy 1967; Hirasawa, Aizu, & Taketani 1969; Takeda, Sato, & Matsuda 1969; Hutchins 1976; Silk 1977; Hartquist & Cameron 1977; Shchekinov & Edelman 1978; Yoshii & Sabano 1979; Tohline 1980; Carlberg 1981; Lepp & Shull 1984; Yoshii & Saio 1986; Lahav 1986; Stahler 1986; Shapiro & Kang 1987; Uehara et al. 1996; Padoan, Raul, & Jones 1997; Nakamura & Umemura 1999,2001,2002; Larson 1995,2000; Abel et al. 1998; Abel, Bryan, & Norman 1999,2000,2002; Bromm, Coppi, & Larson 1999, 2002; Fuller & Couchman 2000; Machacek, Bryan, & Abel 2001). Many authors have examined the possibility of Pop III stars reionizing the universe (e.g., Couchman & Rees 1986; Fukugita & Kawasaki 1994) or partially reionizing the universe (e.g., Gnedin & Ostriker 1997; Gnedin 2000b; Ricotti, Gnedin, & Shull 2001). The primary difficulty for Pop III stars to reionize the universe has by now been realized to be the destruction of H_2 molecules by photons in the Lyman-Werner bands ($11.18 - 13.6$eV; Field et al. 1966; Stecher & Williams 1967) produced by Pop III stars themselves, long before reionization of the universe is complete (Gnedin & Ostriker 1997; Haiman, Rees, & Loeb 1997; Tegmark et al. 1997); H_2 photodissociation time becomes shorter than the Hubble time when the ionizing radiation intensity at the Lyman limit reaches $\sim 10^{-24}$ erg/cm^2/sec/hz/sr at the redshift of interest, about three orders of magnitude below what is required to ionize the universe.

With regard to the initial mass function of Pop III stars a new picture appears to be emerging from a number of recent theoretical studies of the collapse of primordial gas clouds at high redshifts, induced by H_2 cooling. At redshift $z \sim 10 - 30$ primordial gas clouds appear to collapse to form very massive stars with mass $M \geq 100\,M_\odot$, without further fragmentation to take place (Abel et al. 2002; Bromm et al. 2002; Nakamura & Umemura 2002). This outcome is basically determined by the Jeans mass of the collapsing cloud and involves a complicated interplay between cooling and fragmentation. For Pop III galaxies at the redshift in question ($z \sim 15 - 25$) the initial (i.e., interstellar) gas density is less than the threshold value of 10^5 cm^{-3} identified by Nakamura & Umemura (2001,2002) and fragmentation is to occur at low density with fragment mass of $\sim 100\,M_\odot$. We adopt this new theory for Pop III stars. However, we note that most of the main conclusions drawn in this paper will remain as long as the initial mass function of Pop III stars is substantially top-heavy.

We point out two new important sources for X-ray emission in this section, capable of creating a high X-ray background at high redshift to enable the formation of enough H_2

molecules to induce continuous cooling and star formation in minihalos, until the universe is completely reionized.

2.1. X-ray Emission from Pop III Supernova Remnants

We use a simple analytic means to estimate the X-ray emission from Pop III supernova remnants assuming that a spherical supernova blast wave propagates into a uniform density interstellar medium. A spherically expanding supernova remnant at sufficiently late times follows the simple, adiabatic, self-similar Sedov-Taylor solution (Sedov 1959; Taylor 1950; Shklovsky 1968; Cox 1972; Ostriker & Cowie 1981). Specifically, the shock radius (R_s), shock velocity (V_s) and postshock temperature ($T_{\rm s}$) (for $\gamma = 5/3$) obey:

$$R_{\rm s} = 21.7 t_4^{2/5} (E_{52}/n)^{1/5} \text{ pc}, \tag{1}$$

$$V_{\rm s} = 83.9 t_4^{-3/5} (E_{52}/n)^{1/5} \text{ km/s}, \tag{2}$$

$$T_{\rm s} = 8.45 \times 10^6 t_4^{-6/5} (E_{52}/n)^{2/5} \text{ K}, \tag{3}$$

where E_{52} is the explosion energy in 10^{52} ergs, t_4 is the time elapsed since the onset of explosion in 10^4 yr and n is the density of the interstellar medium in cm^{-3}.

The Sedov-Taylor phase ends with a rapid cooling phase, resulting in the formation of a thin dense shell (e.g., Ostriker & McKee 1988). This radiative cooling phase of the shocked gas sets in abruptly approximately when the cooling time is equal to the time elapsed, i.e., when

$$t = \frac{3 n_e k T_{\rm s}}{\Lambda(T_{\rm e}) n_{\rm e}^2}, \tag{4}$$

where 100% hydrogen is assumed in computing the internal energy and the electron density n_e for simplicity (but not for the cooling function Λ; see below); k is the Boltzmann's constant; $n_e = 4n$ is the postshock electron density; $\Lambda(T_e)$ is the volume cooling function for a primordial plasma with 76% hydrogen and 24% in helium by mass, taken from Sutherland & Dopita (1993). We note that the blast waves of the first generation of supernovae propagate into a primordial gas free of metals. Thus metal cooling is non-existent. More importantly, no interstellar dust exists and complex cooling processes due to dust need not to be considered; in particular, X-ray emission would not suffer from dust absorption (Ostriker & Silk 1973; Burke & Silk 1974; Draine & Salpeter 1979; Shull 1980; Wheeler, Mazurek, Sivaramakrishnan 1980; Tielens et al. 1987; Draine & McKee 1993). Combining equations (3,4) and solving for $T_{\rm s}$ as a function of n give results shown in Figure 1, for two cases with $(E_{52}, Z/\,{\rm Z}_\odot) = (3.0, 0.0)$ and $(0.1, 1.0)$, respectively, where the former case may be appropriate for supernovae/hypernovae resulting from very massive Pop III stars (Woosley & Weaver

1982; Ober et al. 1983; Bond et al. 1984; Nakamura et al. 2001; Heger & Woosley 2002) and the latter case for present-day normal supernovae.

A critical point to note is that the density of the general interstellar medium should scale with $(1+z)^3$, being significantly higher at high redshift than that of the local interstellar medium. This assumption should hold in the cosmological context of hierarchical structure formation for the following reasons. First, the mean gas density scales with $(1+z)^3$. Second, halos at low and high redshift in cosmological simulations show similar properties when density and length are measured in their respective comoving units (e.g., Navarro, Frenk, & White 1997; Del Popolo 2001). Third, the spin parameters (i.e., angular momentum distribution) of both high and low redshift halos have very similar distributions peaking at a nearly identical value $\lambda \sim 0.05$ (Peebles 1969; White 1984; Barnes & Efstathiou 1987; Ueda et al. 1994; Steinmetz & Bartelmann 1995; Cole & Lacey 1996; Bullock et al. 2001; Cen et al. 2002). Thus, gas in galaxies at low and high redshift should collapse by a similar factor before rotation support sets in, resulting in interstellar densities scaling as $(1+z)^3$. Direct simulations appear to support this simple analysis (Abel et al. 2002; Bromm et al. 2002). In Figure 1 we have used $n(z) = n_0(1+z)^3$, with $n_0 = 1\mathrm{cm}^{-3}$ being the density of the local interstellar medium, to translate the bottom x-axis (n) to the top x-axis $(1+z)$.

In Figure 1 we see that, at redshift $z = 17$ (or $n = 5832\mathrm{cm}^{-3}$), the blast wave enters the rapid cooling phase at a postshock temperature of 1.0×10^7K. Most of the energy is radiated away during the brief cooling phase (Falle 1975,1981) with photon energy $h\nu \sim kT_\mathrm{s}$, although subsequent evolution of the cooling shell will be subject to various instabilities (e.g., Chevalier & Imamura 1982; Vishniac 1983; Bertschinger 1986; Cioffi, McKee & Bertschinger 1988). Following that, the evolution enters snowplow phase driven by the pressure of a still hot interior gas (McKee & Ostriker 1977; Ostriker & McKee 1988). For a primordial gas cooling at 1.0×10^7K, it is found that $(40\%, 31\%, 18\%)$ of the instantaneously radiated energy is at photon energies above $(0.8, 1.0, 1.5)$keV, respectively. Clearly, a significant amount of the total energy of the supernova blast wave will be turned into X-ray photons. As we will see later, $z = 17$ will be identified as the redshift of the first cosmological reionization by Pop III stars. At higher redshift, the emitted photons from supernova remnant shell cooling would be still harder.

As a consistency check we find that, for $n = 5832\mathrm{cm}^{-3}$, at the onset of the rapid cooling phase, the elapsed time is $t_\mathrm{rad} = 687$ yr, the shell radius is $r_\mathrm{rad} = 1.63$pc, the swept-up interstellar medium mass is $M_\mathrm{rad} = 2594\,\mathrm{M}_\odot$. The fact that M_rad is much larger than the mass of the supernova ejecta ($M_\mathrm{ej} \sim 100\,\mathrm{M}_\odot$) guarantees the Sedov-Taylor solution for the regime in question (until cooling sets in). The fact that the shell radius r_rad is much smaller than the size of galaxies (≥ 10pc) and M_rad is much smaller than the total baryonic mass

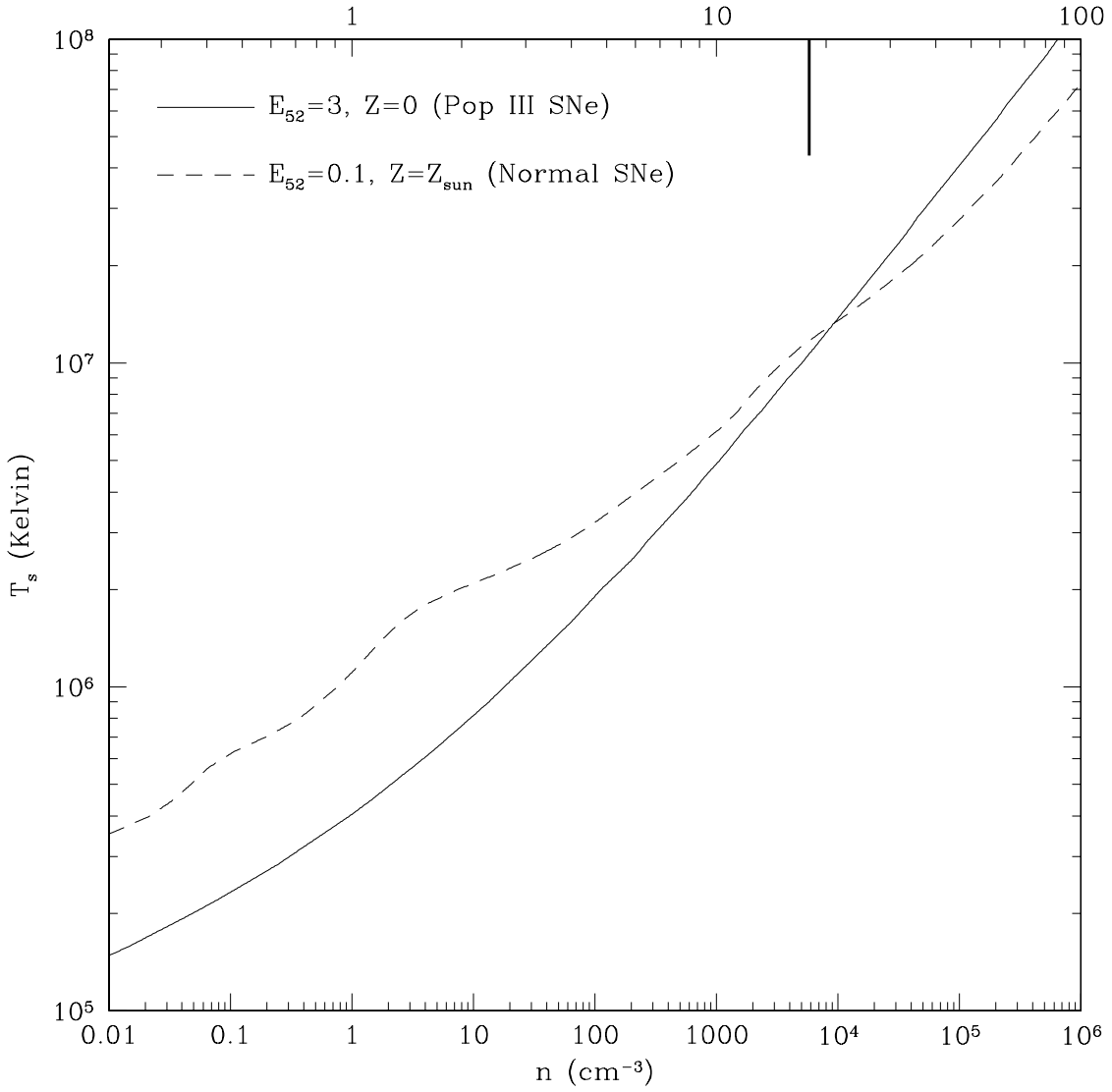

Fig. 1.— The solid curve shows the temperature of the cooling shock front for a supernova/hypernova from a very massive Pop III star with initial energy of 3×10^{52} erg as a function of the interstellar (metal-free) gas density (bottom x-axis) or $1 + z$ (top x-axis). The cooling function assumes a gas of primordial composition. The vertical tick hanging from the top x-axis indicates redshift $z = 17$. Cooling functions are taken from Sutherland & Dopita (1993). As a reference, the dashed curve is for a gas with solar metallicity and a supernova explosion energy of 10^{51} erg, more appropriate for a normal supernova.

in the galaxies ($\geq 10^4\,M_\odot$) in question indicates that the blast wave at the cooling time is still mostly sweeping through high density interstellar medium, as was assumed. As another consistency check, the time required for electrons and ions to reach temperature equilibrium is $t_{\rm eq} = 1.4 \times 10^4 E_{52}^{3/14} n^{-4/7} = 125$ yr for the case considered, which is much shorter than $t_{\rm rad}$, indicating that electrons can radiate away the shock heated thermal energy and that Sedov-Taylor phase is valid. In contrast, in the star-burst model for AGN (Terlevich et al. 1992), the proposed supernova remnants interact with a much higher density medium ($n \sim 10^7 {\rm cm}^{-3}$) such that the Sedov-Taylor phase is never reached due to extremely rapid cooling before thermalization.

In brief, a large fraction of supernova explosion energy in Pop III galaxies at redshift $z \sim 15-25$, possibly as large as $f_{\rm x} \sim 0.30$, is shown to be converted into X-ray photons with energy greater than 1keV. The X-ray background produced by this process will be shown below to be able to play a positive feedback role in the formation of and cooling by H_2 molecules in minihalos.

Let us now proceed to identify the characteristics of the composite spectrum of the background radiation field produced by both emissions from the very massive stars (VMS) and the thermal emission from VMS supernova blast waves. A relevant parameter for our purpose is the ratio of the energy in the Lyman-Werner bands ($h\nu = 11.18 - 13.6$eV) to the energy in photons with $h\nu > 1$ keV, $\Psi_{\rm III} \equiv E_{\rm LW}/E_{>1keV}$. Photons in the Lyman-Werner bands ($11.18 - 13.6$eV) are primarily responsible for photodissociating H_2 molecules and are not heavily absorbed by intervening intergalactic atomic hydrogen (except for the saw-tooth modulation by the atomic Lyman line series; Haiman, Abel, & Rees 2000). Hard X-ray photons at $h\nu > 1$ keV, on the other hand, are also largely unabsorbed by intervening atomic hydrogen and helium and capable of penetrating deeply into the cores of minihalos to produce free electrons through both direct photo-ionization and secondary photo-electron ionization. The abundance of H_2 molecules in the cores of minihalos is primarily a result of the competition between the two. In contrast, photons with energy in the range 13.6eV$-$1keV are heavily absorbed by atomic hydrogen and helium prior to complete reionization of the universe and thus have little effect on the formation of H_2 molecules in the cores of minihalos (see Ricotti, Gnedin, & Shull 2001 for a positive feedback due to ionizing photons on the surface of the expanding HII regions and in relic HII regions). We may write $\Psi_{\rm III}$ approximately as

$$\Psi_{\rm III} \approx \frac{0.007 M_{\rm VMS} c^2 f_{\rm LW}}{\xi_{\rm IMF} E_{\rm ex} f_{\rm x}}, \tag{5}$$

where $f_{\rm LW}$ is the fraction of energy in the Lyman-Werner bands emitted by VMS; c is the speed of light; $M_{\rm VMS}$ is the characteristic mass of VMS ($\sim 200\,M_\odot$; see §3); $E_{\rm ex}$ is the explosion energy of a typical VMS; $\xi_{\rm IMF} < 1$ is inserted to take into account the effect that

some VMS (for example, non-rotating stars with $M \geq 260\,\mathrm{M}_\odot$; Rakavy, Shaviv, & Zinamon 1967; Bond, Arnett, & Carr 1984; Glatzel, Fricke, & El Eid 1985; Woosley 1986) do not produce supernovae (but collapse wholly to a black hole). The supernova explosion energy, $E_{\rm ex}$, released by VMS in the mass range $140 - 260\,\mathrm{M}_\odot$ is approximately $10^{52} - 10^{53}$ erg (Woosley & Weaver 1982; Ober et al. 1983; Bond et al. 1984; Nakamura et al. 2001; Heger & Woosley 2002). The VMS has approximately a blackbody radiation spectrum with an effective temperature of $\sim 10^{5.2}$ K (Tumlinson & Shull 2000; Bromm et al. 2001) for which it is found that $f_{\rm LW} = 1.5 \times 10^{-2}$, yielding

$$\Psi_{\rm III} = 4.2\xi_{\rm IMF}^{-1}(\frac{f_x}{0.3})^{-1}(\frac{E_{ex}}{3\times 10^{52}{\rm erg}})^{-1}(\frac{M}{200\,\mathrm{M}_\odot}). \quad (6)$$

Is it small enough to enhance H_2 formation in minihalos? Let us compare to the results of a systematic study of the effect of X-ray photons on the cooling of minihalo gas by Haiman, Abel & Rees (2000; HAR hereafter). HAR investigated the effect using a $J_\nu \propto \nu^{-1}$ background radiation spectrum, which is cut off at 10 keV. Using Ψ to parameterize their test results, the findings of HAR are that, when

$$\Psi_{\rm HAR} \leq \frac{\ln(13.6/11.18)}{\epsilon_x \ln(10/1)} = 5.1 \quad (7)$$

(for $\epsilon_x = 0.016$), H_2 formation is enhanced and cooling by H_2 is sufficient to allow for the gas in the cores of minihalos with virial temperature $T_{\rm v} \geq 1000$K to collapse to form stars. We note that in evaluating $\Psi_{\rm HAR}$ above we have taken into account a factor of ~ 6 underestimation of $\Psi_{\rm HAR}$ in the original work of HAR due to a factor of 6 underestimation of the LW photon absorption cross section by H_2 molecules (Haiman 2002, private communications; Ricotti, Gnedin, & Shull 2001; Glover & Brand 2002). The correction factor 6 is a lower limit in the optically thin case for H_2 molecules for the cores of minihalos. In the optically thick limit, a substantially larger correction factor needs to be applied (i.e., $\Psi_{\rm HAR}$ would be substantially larger than 5.1), although the exact effect would require a re-calculation of the results in HAR. It thus appears that the X-ray emission from Pop III supernova remnants alone may be able to produce enough X-ray photons relative to the number of photons in the Lyman-Werner bands such that production rate of H_2 molecules dominates over the destruction rate in most of the minihalos.

2.2. X-ray Emission from Miniquasars Powered by Pop III Black Holes

Another consequence of the formation of Pop III stars is an inevitable production of a significant amount of black holes. Pop III stars more massive than $260\,\mathrm{M}_\odot$ would implode

carrying the entire mass to form black holes of about the same mass (Rakavy, Shaviv, & Zinamon 1967; Bond, Arnett, & Carr 1984; Glatzel, Fricke, & El Eid 1985; Woosley 1986) without producing explosions. Pop III stars less massive than $140\,\mathrm{M}_\odot$ would in the end explode as supernovae or hypernovae leaving behind black holes of mass $\sim 10 - 50\,\mathrm{M}_\odot$ (Heger & Woosley 2002). Both kinds of black holes should form nearly instantaneously (a few million years after the formation of the stars). These Pop III black holes could accrete gas from surroundings and become miniquasars. The probability of gas accretion onto these black holes is at least as high as in their lower redshift counterparts since the gas density is higher and halos have lower spins at high redshift. In the case of the very massive Pop III black holes ($M \geq 260\,\mathrm{M}_\odot$) formed without explosion, gas may be ready to accrete immediately, since the surrounding gas has not been blown away. The dynamics of the black holes in these environments in the context of cosmological structure formation is by itself a complex subject and will only be treated in separate works. Here we make the assumption that these black holes would accrete gas and grow.

The characteristic gas temperature of a disk powered by accretion onto a black hole is (Rees 1984):

$$T_{\mathrm{E}} = 1.3 \times 10^7 M_2^{-1/4}\ K, \tag{8}$$

where M_2 is the black mass in $10^2\,\mathrm{M}_\odot$. For $M_{\mathrm{BH}} = (200, 20)\,\mathrm{M}_\odot$, we have $T_{\mathrm{E}} = (1.3 \times 10^7, 2.4 \times 10^7)$ K. While the spectral energy distribution (SED) of quasars powered by supermassive black holes is known to contain a significant fraction in X-rays (e.g., Elvis et al. 1994), the miniquasars at high redshift powered by much smaller black holes are conspicuous in X-rays, probably emitting predominantly in X-ray band from both thermal and nonthermal emission. A somewhat more quantitative argument may be made as follows. The SED of quasars powered by supermassive black holes of mass $\sim 10^8\,\mathrm{M}_\odot$ contains a substantial amount of energy in the X-rays but the largest concentration of energy appears to peak at $\sim 12 - 13$eV (UV bump; Elvis et al. 1994) barring the unknown gap between UV and X-ray. Under the assumption that the SED peak frequency scales with the characteristic temperature T_{E}, then the peak frequency for Pop III black hole powered miniquasars would be shifted (by a factor of ≥ 100 compared to quasars) to $h\nu \geq 1$keV.

Let us now compute the X-ray background produced by miniquasars powered by Pop III black holes. We put this quantitatively in the context of the ratio of energy in LW photons to that of X-ray photons. First, an order-of-magnitude estimate. If a miniquasar has accreted a fraction, η_Q, of the initial mass of the black hole, the radiated energy will be

$$E_Q = \eta_Q \alpha c^2 M_{BH}, \tag{9}$$

where α is the radiative efficiency. Then, the ratio Ψ may be written as

$$\Psi_Q = \frac{0.007c^2 f_{\rm III} f_{\rm LW}}{0.1\alpha_{0.1}c^2\eta_Q f_{\rm III} f_{\rm BH} f_{\rm Xray} f_{\rm esq}} = 10^{-3}\eta_Q^{-1}\alpha_{0.1}^{-1} f_{BH}^{-1} f_{\rm Xray}^{-1} f_{\rm esq}, \quad (10)$$

where $f_{\rm III}$ is the fraction of mass collapsed into Pop III stars; $f_{\rm BH}$ is the fraction of mass in $f_{\rm III}$ that ends in black holes; $\alpha_{0.1}$ is radiative efficiency of the miniquasars in units of 0.1; $f_{\rm Xray}$ is the fraction of energy radiated by miniquasars with photon energy greater than 1 keV; $f_{\rm esq}$ is the X-ray escape fraction from miniquasars; we use $f_{\rm LW} = 1.5 \times 10^{-2}$. The value of $\alpha_{0.1}$ is thought to be close to unity (Rees 1984) and the value of $f_{\rm Xray}$ is expected to be of order unity. The fraction of mass in Pop III stars ultimately collapsing to black holes $f_{\rm BH}$ is also of order unity, if either Pop III stars are very massive $\sim 100\,{\rm M}_\odot$ or much more massive than local stars (with normal IMF) $\gg 1\,{\rm M}_\odot$. The accretion fraction η_Q would depend on the gas accretion rate and the formation time of the black hole; parameterization by Equation (10) would be fairly accurate if black holes formed long time ago. But a more accurate way to compute the X-ray energy from miniquasars is to integrate over time over all miniquasars by parameterizing each radiating at $\xi_{\rm Edd}$ times the Eddington luminosity. The results are shown in Figure 2, where the solid and dotted curves show $\Psi_{\rm Q}$ with radiative efficiency of $\alpha = (0.1, 0.03)$, respectively. The global Pop III star formation rate is computed using Press-Schechter (1974) formula considering all halos with virial temperature greater than 200 K, below which H_2 cooling decreases sharply (see §3). The reason that the dotted curve with lower radiative efficiency ($\alpha = 0.03$) lie below (i.e., emits more X-ray photons than) the solid curve is that the black hole mass in this case grows at a faster rate, being inversely proportional to the radiative efficiency.

Another useful way to estimate the growth of mass in black holes is to follow the local observed black hole mass-bulge mass relation, $M_{\rm BH} \sim 0.006 M_{\rm bulge}$, (Magorrian et al. 1998). If the same ratio of the mass in black holes to bulge mass, which at high redshift may be equated to the total stellar mass, holds at high redshift, then we can readily compute the energy liberated by gas accretion onto Pop III black holes as

$$\Psi_{\rm Q} = \frac{0.007c^2 f_{\rm III} f_{\rm LW}}{0.006 \times 0.1\alpha_{0.1}c^2 f_{\rm III} f_{\rm BH} f_{\rm Xray} f_{\rm esq}} = 0.88\alpha_{0.1}^{-1}\left(\frac{f_{\rm esq}}{0.2}\right) f_{BH}^{-1} f_{\rm Xray}^{-1}. \quad (11)$$

The horizontal dashed line in Figure 2 indicates $\Psi_{\rm Q}$ computed this way with radiative efficiency of $\alpha = 0.1$ and X-ray escape fraction $f_{\rm esq} = 0.2$.

From Figure 2 it is evident that Ψ_Q is significantly smaller than $\Psi_{HAR} = 5.1$ (Equation 7), at $z \leq 20$, required to induce sufficient H_2 cooling in minihalos (HAR). The higher value of $\Psi_{\rm Q}$ at higher redshift ($z \geq 20$) is due to the fact that the age of the universe becomes much shorter than the Eddington time of $\sim 4 \times 10^8$ yr and the black holes have not had

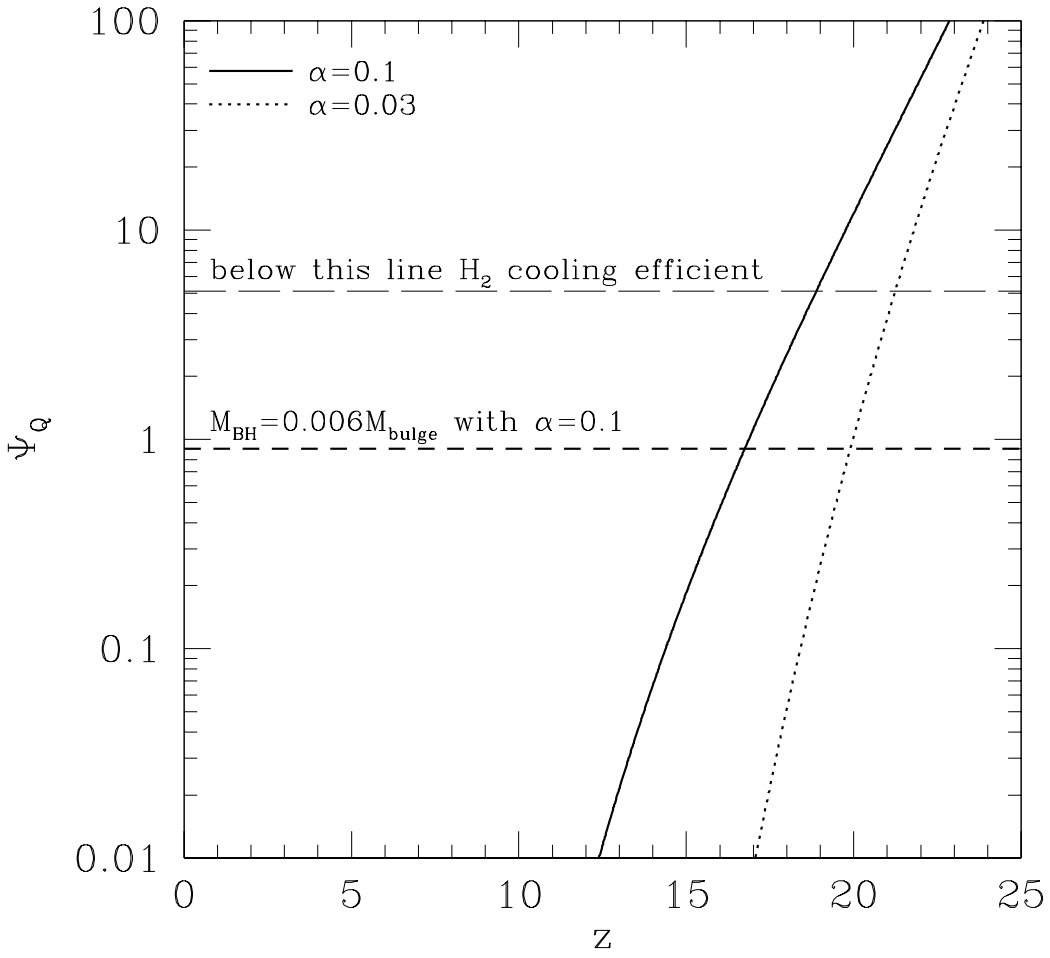

Fig. 2.— The solid and dotted curves show $\Psi_{\rm Q}$ as a function of redshift, by integrating over time the miniquasar luminosity radiating at Eddington luminosity with radiative efficiency of $\alpha = (0.1, 0.03)$, respectively. The horizontal dashed line indicates the case if one adopts the local observed black hole mass-bulge mass relation (Magorrian et al. 1997) with radiative efficiency of $\alpha = 0.1$. The horizontal long-dashed line indicates the required value (HAR), below which H_2 cooling is efficient. $\Psi_{\rm Q}$ would scale with $\xi_{\rm Edd}$ and $f_{\rm BH}^{-1} f_{\rm Xray}^{-1}$, for both of which we have assumed value of unity. We also assume that 20% ($f_{\rm esq} = 0.2$) of the soft X-ray radiation (~ 1 keV), averaged over all miniquasars, escapes to the intergalactic space; this value is based on observations of AGN and quasars at lower redshift (Brandt 2002, private communications). We have ignored cosmological redshift and dilution effects in this illustration.

enough time to accrete a substantial amount of gas; the age of the universe is 1.9×10^8 yr at $z = 20$ (for $H = 70$ km/s/Mpc, $\Omega_M = 0.25$, $\Lambda = 0.75$).

In summary, two distinctive mechanisms, namely supernova remnants and miniquasars, each appears to be able to generate enough X-ray emission at $z \sim 15-20$ to provide positive feedback on star formation in subsequent (other) minihalos by making a sufficient number of X-ray photons relative to the number of destructive photons produced in the Lyman-Werner bands. The combination of the two should ensure that enough X-ray radiation is produced as a result of Pop III star formation. In addition, there may be other, significant X-ray emission mechanisms such as inverse Compton emission (e.g., Hogan & Layzer 1979; Oh 2001) or massive X-ray binaries (e.g., Bookbinder et al. 1980; Helfand & Moran 2001). Moreover, additional positive feedback mechanisms, such as that proposed by Ferrara (1998) due to enhanced H_2 formation in the supernova cooling shells and that put forth by Ricotti, Gnedin, & Shull (2001) from the enhanced H_2 formation at the surfaces of Strömgren spheres of individual Pop III galaxies, will further help promote H_2 formation. This removes the chief obstacle to continuous formation of Pop III stars. Thus, Pop III stars will continue to form until the universe is completely reionized, whose epoch will be computed next in §3.

Since the assumption that X-ray emission produced by these two processes related to Pop III star formation can produce positive feedback to subsequent star formation is essential, it is warranted to have independent checks. We will compare our results to Glover & Brand (2002; GB hereafter). We compare to their X-ray emission model due to inverse Compton, which has luminosity density $L_{\rm X} = 7.7 \times 10^{23}(\nu_0/\nu) f_{\rm e}$ erg s^{-1}Hz^{-1}(M$_\odot$yr^{-1})$^{-1}$, where $\nu_0 = 1$keV and $f_{\rm e}$ is the fraction of supernova energy transferred to relativistic electrons. Integrating $L_{\rm X}$ over a range $1-10$keV we obtain $E_{\rm X} = 4.28 \times 10^{41} f_{\rm e}$ erg s^{-1}(M$_\odot$yr^{-1})$^{-1}$. The luminosity at the Lyman-Werner bands in GB is $L_{\rm LW} = 1.1 \times 10^{28}$erg s^{-1} Hz^{-1}(M$_\odot$yr^{-1})$^{-1}$, which after integration over Lyman-Werner bands gives $E_{\rm LW} = 6.4 \times 10^{42}$erg s^{-1} (M$_\odot$yr^{-1})$^{-1}$. Taking the ratio of the above two luminosities yields $\Psi_{\rm GB} \equiv E_{\rm LW}/E_{\rm X} = 150$, for the most optimistic model that they use with $f_{\rm e} = 0.1$. For this model GB find that the critical virial temperature of halos where cooling is sufficient is lowered from 8×10^3K to about $(2-3) \times 10^3$K at $z \sim 17$ (see Figure 6 in GB), a significant effect. While even this model is already sufficient to enable molecular cooling in halos with $T_v > 2000$K to reionize the universe at $z \sim 17$ (see Figure 5 below), it is expected that the much smaller $\Psi_{\rm III}$ computed above for Pop III stars in our model would further drive the critical virial temperature to much lower values and enable star formation in almost all minihalos, consistent with the conclusions reached by HAR.

3. First Cosmological Reionization

The emission spectrum of metal-free VMS with $M \geq 100\,\mathrm{M}_\odot$ is relatively simple and has, to a very good approximation, a blackbody spectrum with an effective temperature of $\sim 10^{5.2}$ K. For our purpose we can simply assume that a VMS radiates at the Eddington luminosity $L_{\rm Edd} = 1.3{\times}10^{38}(M/\,\mathrm{M}_\odot)\mathrm{erg\,s}^{-1}$ for about $3{\times}10^6$ yr (El Eid, Fricke, & Ober 1983; Bond, Arnett, & Carr 1984; Bromm, Kudritzki, & Loeb 2001; Schaerer 2002). With the high effective temperature VMS are efficient emitters of ionizing photons with approximately ten times more hydrogen ionizing photons per unit stellar mass than stars with a normal IMF. We will compute the epoch of the first reionization by Pop III stars, assuming that Pop III stars can continuously form in minihalos, as validated in §2.

The gas fraction in halos above a given temperature (or mass, M) at redshift z is obtained using the Press-Schechter (1974) formula:

$$\psi(>M,z) = \mathrm{erfc}(\frac{\delta_c}{\sqrt{2}\sigma(M,z)}) \tag{12}$$

where erfc() is the complimentary error function and $\sigma(M,z)$ is the rms density fluctuation smoothed over a region of mass M at redshift z; δ_c is a constant equal to 1.69 indicating the amplitude of the density fluctuations on a top-hat sphere that collapses at redshift z (Gunn & Gott 1972). The halo mass within the virial radius M is related to the virial temperature at redshift z by the standard formula:

$$M_{\rm v} = 1.2\times10^3(\frac{\Omega_{\rm M}}{0.2})^{1/2}(1+z)^{-3/2}T_{\rm v}^{3/2}\,\mathrm{M}_\odot, \tag{13}$$

where $T_{\rm v}$ is the virial temperature in Kelvin and $\Omega_{\rm M}$ is the matter density at redshift zero in units of the closure density. Figure 3 shows the fraction of gas in halos as a function of redshift, with virial temperatures greater than the five indicated values, $T_v = (200, 1000, 2000, 4000, 8000)$K. Figure 4 relates the virial temperature at each redshift to the halo mass for the five indicated virial temperatures.

We identify the epoch of the first reionization with the time when the global ionizing photon production rate in Pop III stars exceeds the global recombination rate. The global recombination rate depends linearly on the effective clumping factor of ionized gas, C, which is uncertain and in turn depends on several factors including the overall density fluctuations and radiation shielding. Thus, we will, tentatively, treat C as a free parameter and then examine its likely range and the dependence of the results on its value. The global Pop III star formation rate is computed using Equation (11) considering all halos with virial temperature greater than 200 K (the top curve in Figure 3), below which H_2 cooling decreases sharply. (Note that the Jeans mass for a gas which has cooled adiabatically since recombination is

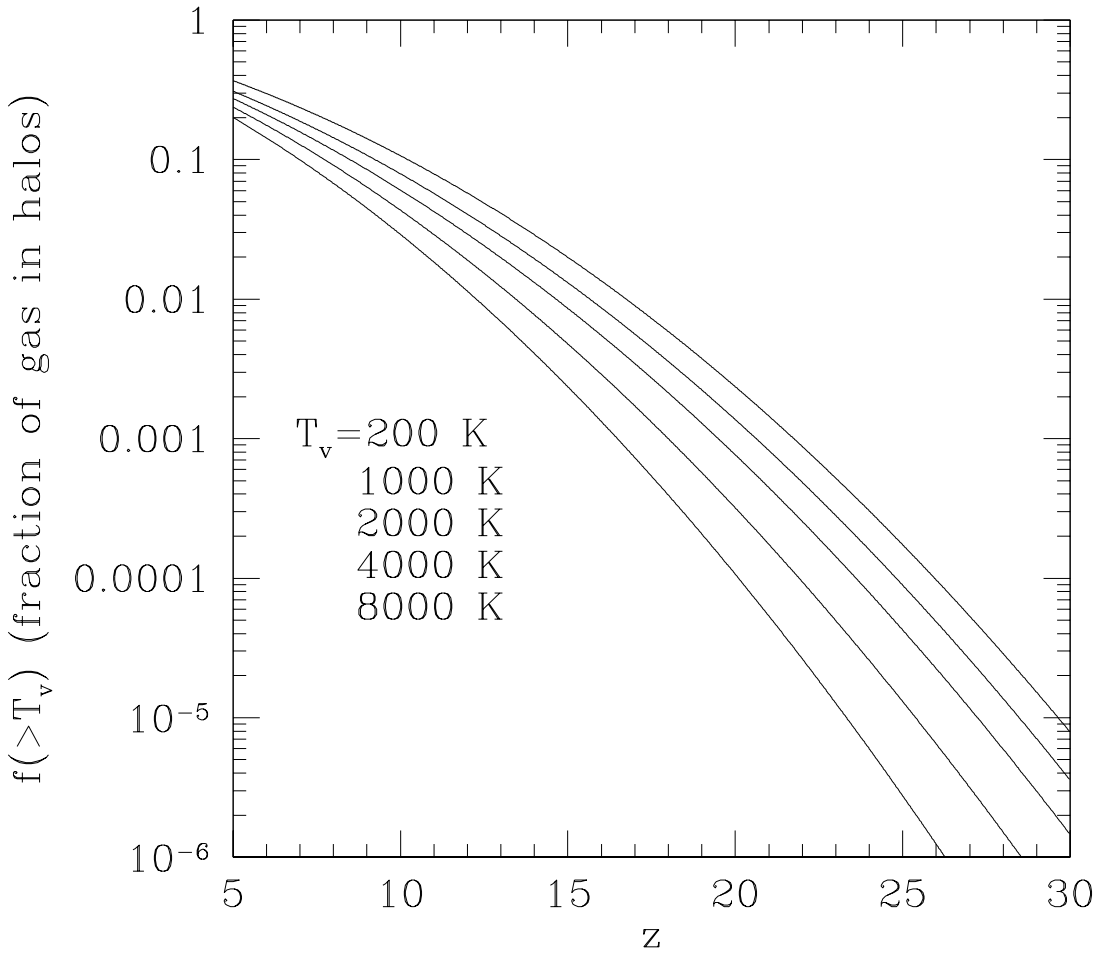

Fig. 3.— shows the fraction of gas in halos as a function of redshift, for five indicated virial temperatures, $T_v = (200, 1000, 2000, 4000, 8000)$K.

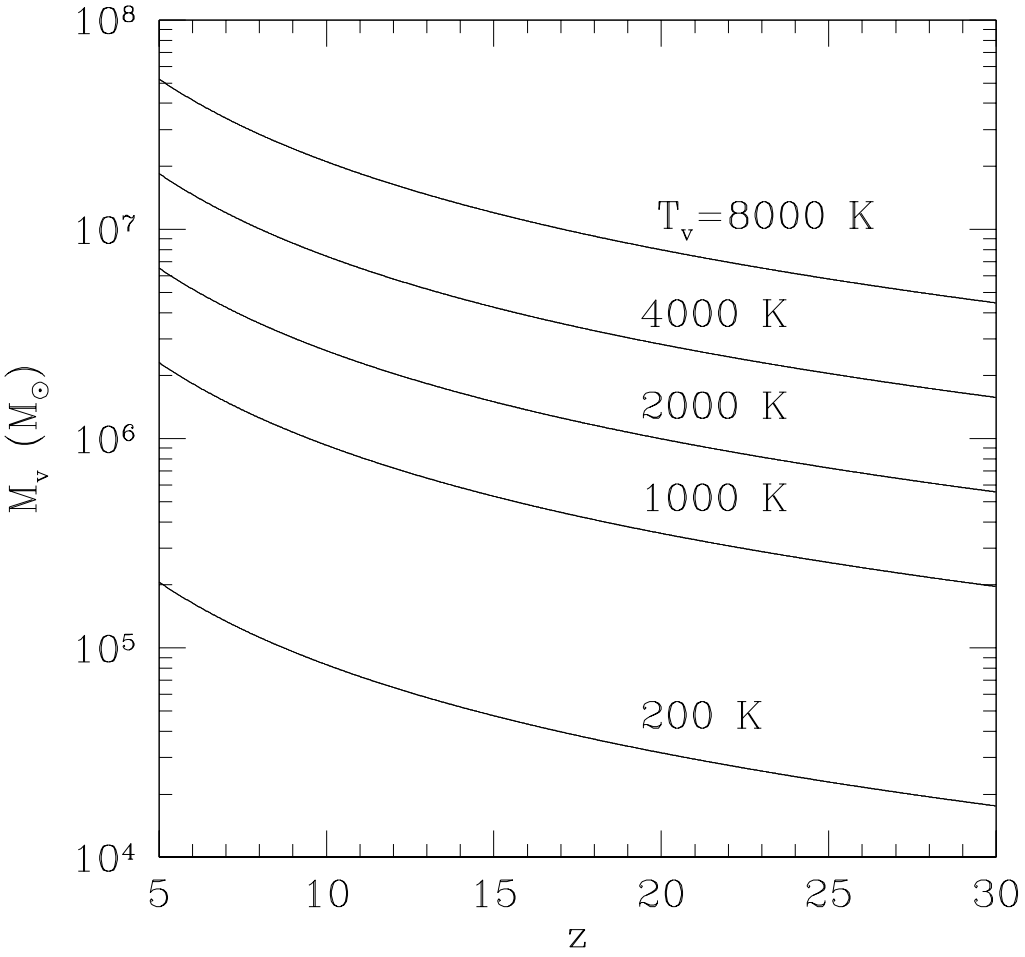

Fig. 4.— Relates the virial temperature to the mass of the halo as a function of redshift, for five indicated virial temperatures, $T_v = (200, 1000, 2000, 4000, 8000)$K.

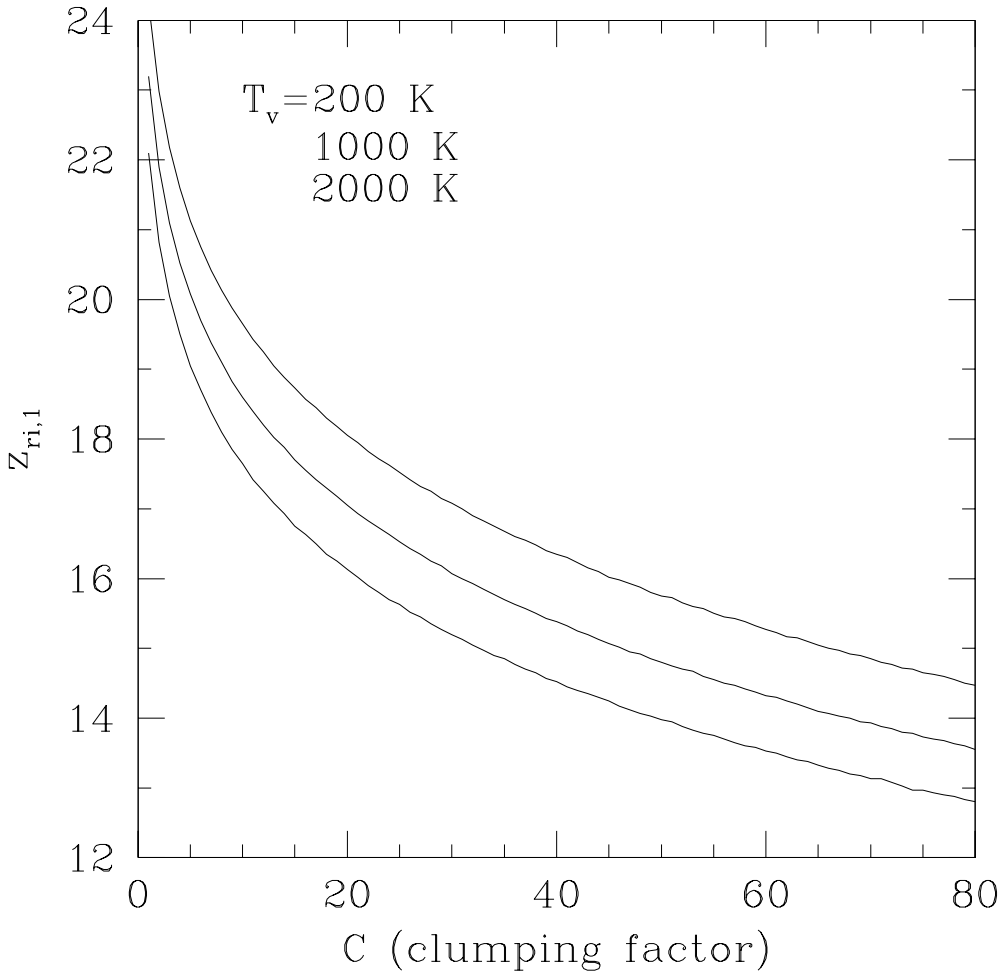

Fig. 5.— The redshift of the completion of the first reionization as a function of the clumping factor. We used $c_1^* = 0.01$ and $\omega_{\rm IMF} = 0.5$. Hydrogen mass fraction of the primordial gas of 76% is assumed. Hydrogen recombination coefficient of $2.5 \times 10^{-13}{\rm cm}^3$ s^{-1} is used for an ionized gas of temperature 2×10^4 K.

much smaller than the mass of a halo with virial temperature equal to 200 K at the redshifts of interest here.) But it is seen that, as indicated in Figure 3, a higher mass cutoff does not significantly change the results. We allow a fudge factor, $\omega_{\rm IMF} \leq 1$, to characterize the unknown IMF of Pop III stars which may contain some fraction of stars less massive than $\sim 100\,{\rm M}_\odot$ emitting hydrogen ionizing photons somewhat less efficiently. We use a fairly conservative star formation efficiency for first generation stars, $c_1^* = 0.01$, the fraction of gas formed into stars out of an amount of gas virialized in minihalos.

Adopting the hydrogen ionizing photon production rate of 1.6×10^{48} photons ${\rm s}^{-1}$ ${\rm M}_\odot{}^{-1}$ for VMS (Bromm et al. 2001), we obtain results shown in Figure 5. We see that the universe will be ionized by Pop III stars at redshift $z_{ri,1} = 14 - 24$, depending on the actual clumping factor. We note that the clumping factor at high redshift $z \geq 15$ is expected to be small, ~ 5 (Haiman, Abel, & Madau 2001). We choose $z_{ri,1} = 17$ for further analyses. However, the conclusions drawn do not sensitively depend on the actual value of $z_{ri,1}$ given the allowed range $z = 14 - 20$, where the lower bound $z = 14$ follows Figure 5 and the upper bound $z = 20$ is dictated by the requirement for H_2 cooling (Figure 2). It is found that for $c_1^* = 0.01$ about 6.6 hydrogen ionizing photons per baryon have been produced by $z = 17$. We note that, had a higher temperature cutoff of 2000 K used instead of 200 K, $z_{ri,1} = 17$ is still reasonable if $C \leq 10$, as supported by simulations (Haiman, Abel, & Madau 2001).

Finally, we point out that the ratio of the energy in hydrogen ionizing photons emitted by Pop III stars to the energy emitted by miniquasars will be $\Psi_Q^{-1} f_{\rm LW}^{-1}$, which is significantly larger than unity. Thus, the first reionization is accomplished by Pop III stars, not the miniquasars of Pop III black holes.

4. Second Cosmological Recombination and Second Cosmological Reionization

After the universe was first reionized and heated to a temperature of $\geq 10^4$ K at $z = 17$, the gas in minihalos will be either driven out by photoheating due to internal or external ionizing radiation on a dynamic time scale ($\sim 10^7$ yr) (Shapiro, Raga, & Mellema 1997; Barkana & Loeb 1999) or blown away by supernova explosions (Mac Low & Ferrara 1999; Mori, Ferrara & Madau 2002). The Jeans mass increases by about three orders of magnitude. Since a vast majority of the star formation activities occuring then is in minihalos with virial temperature much lower than $\sim 10^4$ K, the star formation rate suffers a sharp drop in the immediate aftermath of the first reionization. The subsequent evolution is somewhat more complicated and requires some careful treatment.

In this section we will examine the evolution of the IGM subsequent to the first reion-

ization at $z_{ri,1} = 17$, until the universe is completely reionized for the second time at $z \sim 6$, as indicated by recent observations (e.g., Fan et al. 2001; Becker et al. 2001, Barkana 2001; Cen & McDonald 2002). We will defer a brute-force calculation for a later work. Instead, we will use a new, simple Monte Carlo-like approach to economically obtain the results, which we hope should be capable of capturing the essential physical processes involved.

At any time after the first reionization the gas in the universe consists of N distinct regions in the phase space specified by (T_i, y_i), where T_i and y_i are the temperature and neutral hydrogen fraction, respectively. Each region contains f_i fraction of the total gas in the universe and the mean gas density is assumed to be equal to the global mean; the sum of all f_i is unity. For each region i we solve a combined set of equations simultaneously to follow the evolution of gas and star formation:

$$\frac{df_i}{dt} = -\frac{dN_{ion}}{dt}\frac{1}{\bar{n}\bar{y}}f_i, \tag{14}$$

$$\frac{dT_i}{dt} = -\frac{\Sigma_i(T_i, y_i, C_i)}{3k}, \tag{15}$$

$$\frac{dy_i}{dt} = \alpha C_i \bar{n}(1-y_i)^2 - \beta C_i \bar{n} y_i (1-y_i), \tag{16}$$

where $\bar{n}$ is the global mean gas number density; $\bar{y}$ is the global average of the neutral hydrogen fraction; Σ_i is the net cooling rate per unit mass (including Compton cooling, atomic line cooling, recombination cooling, photoheating due to ionization and adiabatic cooling due to cosmic expansion), which is a function of T_i, y_i, clumping factor C_i (see below) and redshift z; k is the Boltzmann's constant; α is the case B hydrogen recombination coefficient; N_{ion} is the number of ionizing photons per unit volume, equal to

$$\frac{dN_{ion}}{dt} = \frac{c_2^* \epsilon_{UV} c^2 \bar{\rho} f_{\rm es}}{13.6{\rm eV}}\frac{d\psi}{dt} \tag{17}$$

where c_2^* is the star formation efficiency for second generation stars; ϵ_{UV} is the fraction of energy (in units of rest mass of stars formed) turned into ionizing photons; c is the speed of light; $\bar{\rho}$ is the global mean gas mass density; $f_{\rm es}$ is the ionizing photon escape fraction from galaxies; $\frac{d\psi}{dt}$ is the global rate of fraction of gas formed into stars, equal to

$$\frac{d\psi}{dt} = \sum_{i=1}^{N} f_i \frac{d\psi_i}{dt}, \tag{18}$$

where $\frac{d\psi_i}{dt}$ is the rate of the fraction of gas formed into stars in region i. At each time step, we use the Press-Schechter formula to compute the fraction of gas, ψ_i, that is in halos to form stars in region i (Equation 12); this fraction depends on the temperature of the IGM

of region i, i.e., only those halos whose mass is greater than the Jeans mass given the IGM temperature of region i at that time will contribute to the star formation at that time step. We use the formula in Peebles & Dicke (1968),

$$M_J = 4.38 \times 10^4 \Omega_M^{-1/2} T_i^{1.5} (1+z)^{-1.5} \tag{19}$$

for the Jeans mass, which is used as the threshold in Equation (12). The clumping factor in each region i is $C_i = \psi_i C_{\rm halo} + (1 - \psi_i)$, where $C_{\rm halo}$ is the effective clumping factor of virialized gas and the remaining gas is are assumed to have a clumping factor equal to unity. We will adjust $C_{\rm halo}$ such that the overall C of the universe matches simulations. Equation (14) is simply the rate that mass in region i is being ionized by stars. The sum of ionized gas over all the phase space regions at each time step creates a separate region in the phase space with $T_{N+1} = 2 \times 10^4$ K and $y_{N+1} = 10^{-4}$ (results obtained do not depend on the exact choice for the value of the initial neutral fraction of photoionized gas) with an initial mass fraction equal to

$$f_{N+1} = \frac{dN_{ion}}{dt} \frac{1}{\bar{n}\bar{y}} \Delta t, \tag{20}$$

where Δt is the time step. We assume that all regions in the phase space co-exist in real space when averaged over a sufficiently large volume and photoionization ionizes all phase space regions uniformly, as indicated by Equation (14).

As the initial condition we assume that, immediately after the first reionization at $z_{ri,1}$, all gas in halos (dominant fraction of those are minihalos) is driven out into the intergalactic space either by (internal or external) photoheating or by supernova winds. In reality there may be a slight delay of order $\sim 10^7$ yr in the case of photo-evaporation due to a finite outflow velocity of ~ 10 km/s; in the case of supernova winds, the delay time will be still shorter. Since the Hubble time at $z = 17$ is 2.4×10^8 yr, the assumption of instantaneous outflow is fairly good. For simplicity we set $T_1 = 3 \times 10^4$ K [the results of the calculation do not change significantly if different T_1 is used within a reasonable range $(1.5 - 4) \times 10^4$K], $y_1 = 1 \times 10^{-4}$, $C_1 = 1$, $f_1 = 1$ at $z = z_{ri,1} = 17$ and the initial number of entries in the phase space (T, y) is $N = 1$. N increases linearly with the number of time steps taken. We can afford to make the timesteps sufficiently small to be able to follow the ionization and energy equations accurately in this simple approach.

The attentive reader may have noticed the central idea behind this simple approach. That is, this approach attempts to mimick the percolation process of the reionization, where individual HII regions are created and their subsequent evolution are followed, until HII regions completely fill up the entire space, marking the end of the reionization. For this reason we do not include a photoionization term on the right hand side of Equation (16). Needless to say, this method is highly simplified. More sophisticated calculations would

require simulations that follow detailed three-dimensional radiative transfer (e.g., Norman, Paschos, & Abel 1998; Abel, Norman, & Madau 1999; Razoumov & Scott 1999; Kessel-Deynet & Burkert 2000; Gnedin & Abel 2001; Cen 2002) but will be carried in our future work.

Another assumption that we make in the calculations is that, like the Pop III star formation, star formation continues in all halos where gas is able to collect, not limited to larger halos where atomic hydrogen cooling becomes efficient. While the IGM may have been enriched by metals ejected from Pop III supernovae, the low mean metallicity of $Z \sim 10^{-3}\,\mathrm{Z}_\odot$ makes metal cooling at low temperature still insufficient. At lower redshift ($z \leq 10$), the supernova blast waves are no longer emitting a significant fraction of the cooling energy in X-rays due to a combined effect of lower interstellar medium density and lower supernova explosion energy. X-ray emission from miniquasars powered Pop III black holes will continue, provided accreting gas demand is supplied. Black holes formed due to second generation of stars of (more or less) normal IMF would only contribute a small fraction to the total black hole mass, since only a very small fraction of total stellar mass would end up in black holes ($\leq 10^{-3}$ for normal IMF versus ~ 1 for Pop III). However, even in the absence of the X-ray background, a high residual ionization fraction can be maintained after the first reionization, thanks to the long hydrogen recombination time. Let us make a simple estimate by computing the ratio of the recombination time to the dynamical time of a region of overdensity δ with ionization fraction x. We find

$$\frac{t_{\rm rec}}{t_{\rm dyn}} = 0.8(\frac{1+z}{16})^{-3/2}(\frac{\delta}{10^5})^{-1/2}(\frac{x}{10^{-2}})^{-1} \tag{21}$$

for $T = 5000$ K. It is thus evident that an ionization fraction of order $10^{-3} - 10^{-2}$ will be maintained for δ as high as 10^5 (the core density is about $\delta = 10^4 - 10^5$), adequate to enable the formation of a sufficient amount of H_2 molecules to supply ample cooling at $T \leq 10^4$K (HAR; Tegmark et al. 1997). With additional help from the still significant X-ray background, star formation should continue to take place in any halo where gas is able to accumulate. Looking forward to the results, it turns out that the condition for molecular cooling has negligible effect, since intergalactic gas can not accumulate onto halos with virial temperature less than 10^4K.

Let us now turn to the results. Figure 6 shows the global hydrogen neutral fraction and the complimentary ionized fraction as a function of redshift from the first reionization redshift $z = 17$ to the second reionization redshift $z \sim 6$. We use $c_2^* = 0.05$, $C_{\rm halo} = 30$, $f_{\rm es} \times e_{\rm UV} = 5.4 \times 10^{-6}$ (see Equation 17). The value of $C_{\rm halo} = 30$ is chosen so as to produce the overall clumping factor (see Figure 8) in reasonable agreement with numerical simulation. The star formation efficiency is less constrained but the chosen value is consistent

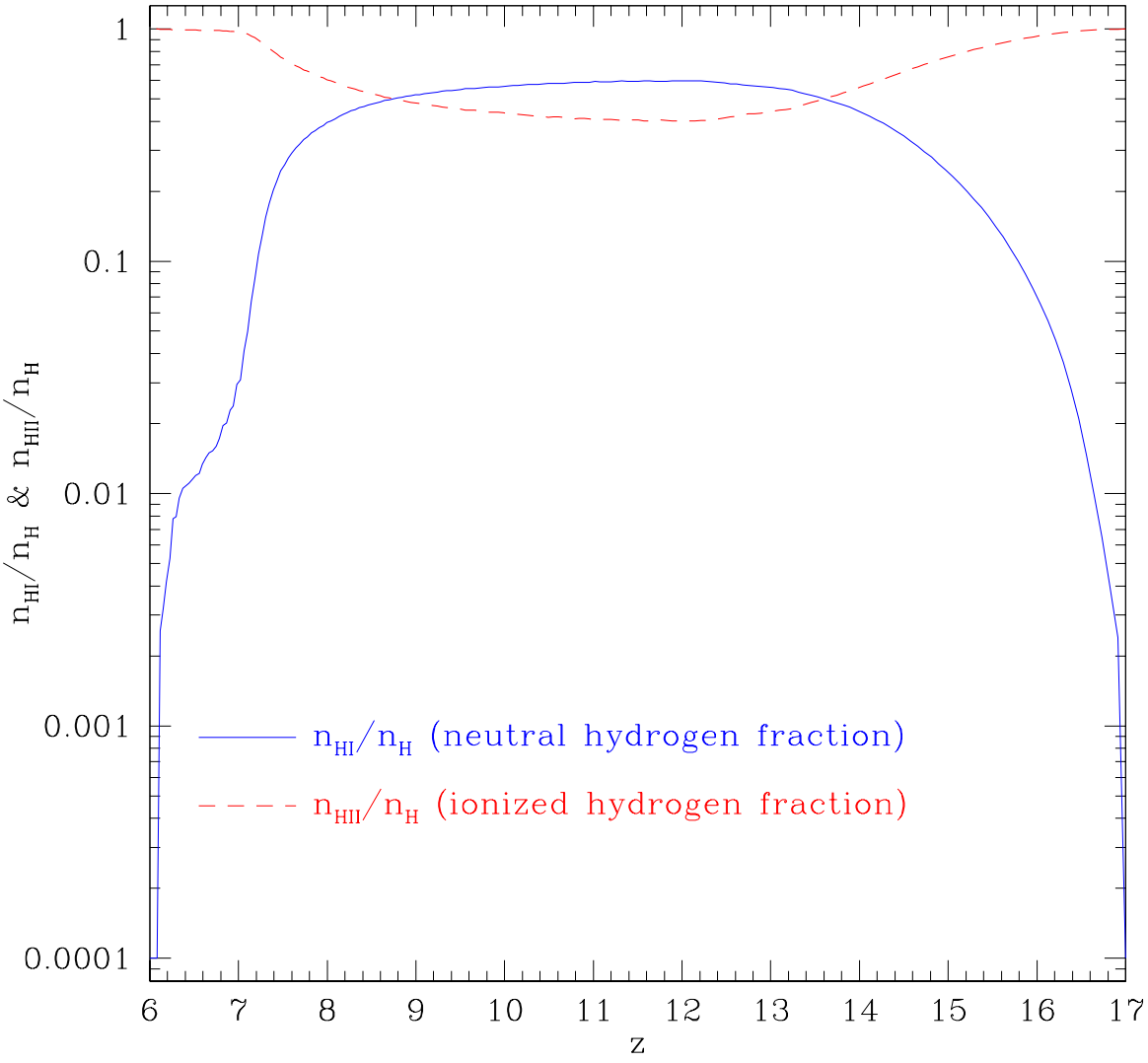

Fig. 6.— shows the global mean of the hydrogen neutral (solid) and complimentary ionized (dashed) fraction as a function of redshift, since the first reionization at $z = 17$. We use $c_2^* = 0.05$, $C_{\rm halo} = 30$, $f_{\rm es} \times e_{\rm UV} = 5.4 \times 10^{-6}$.

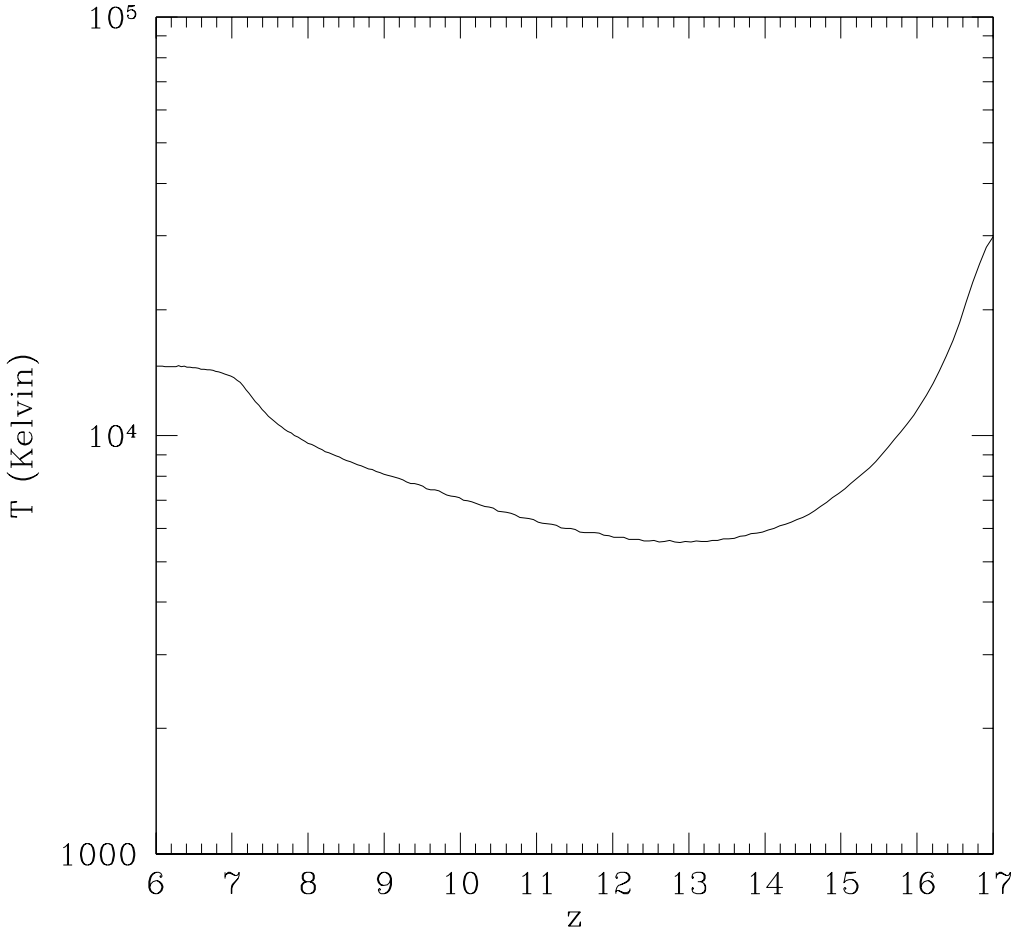

Fig. 7.— shows the evolution of the mean IGM temperature as a function of redshift during the second cosmological reionization process.

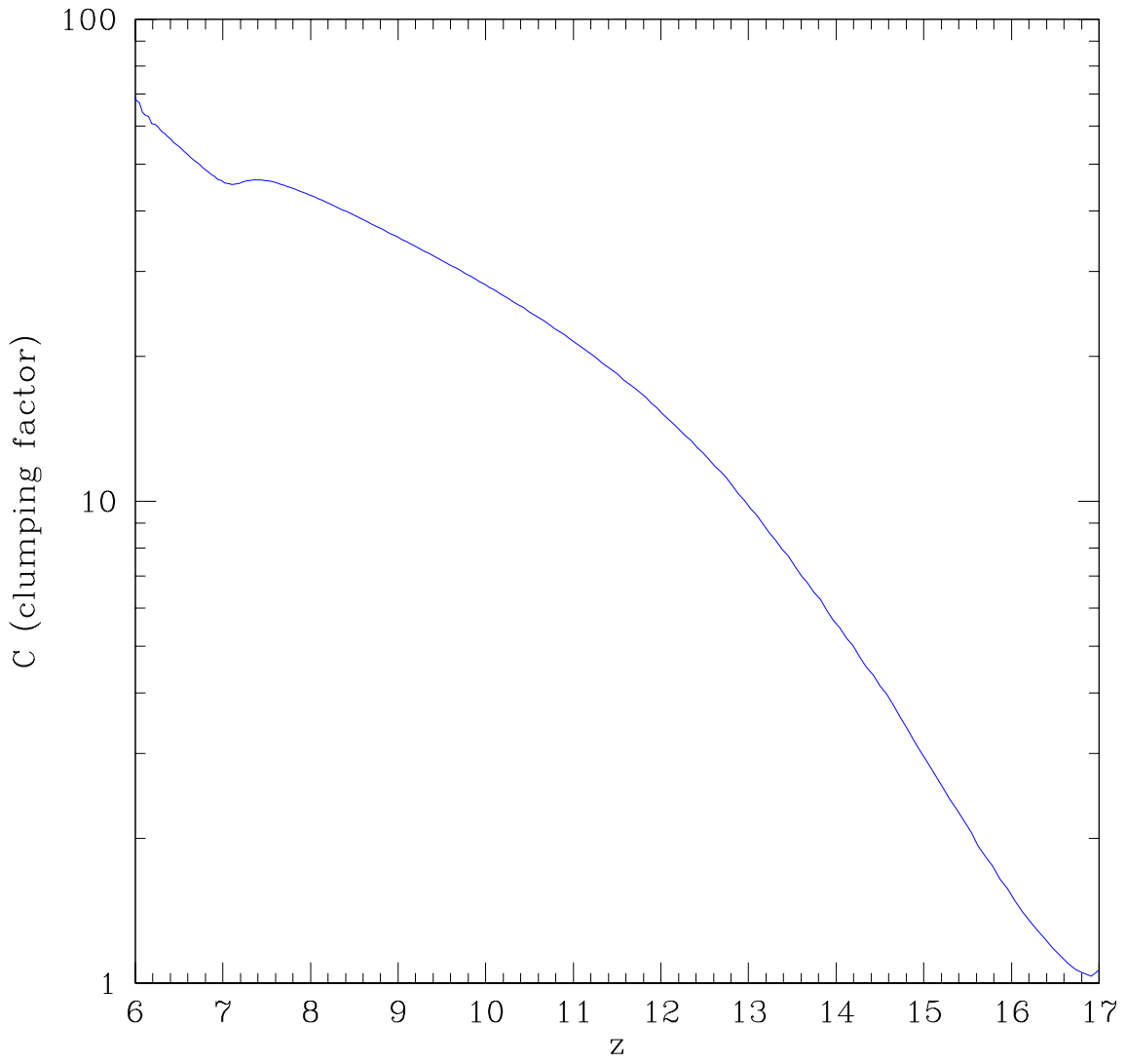

Fig. 8.— shows the evolution of the mean clumping factor as a function of redshift during the second cosmological reionization process, consistent with direct numerical simulation of Gnedin & Ostriker (1997).

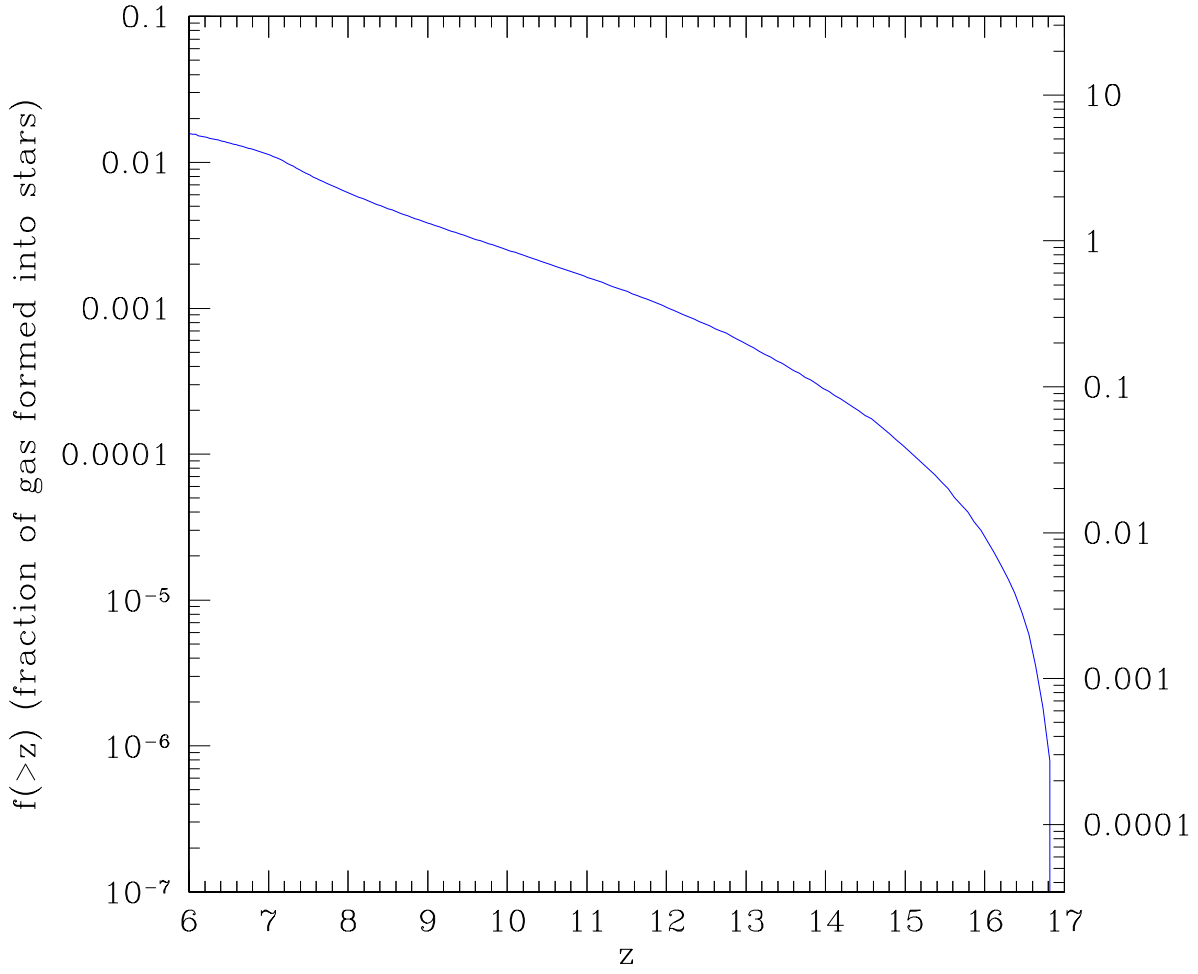

Fig. 9.— The left y-axis shows the evolution of the fraction of gas formed into stars as a function of redshift. The right y-axis translates the fraction of gas formed into stars into the number of ionizing photons per baryon as a function of redshift.

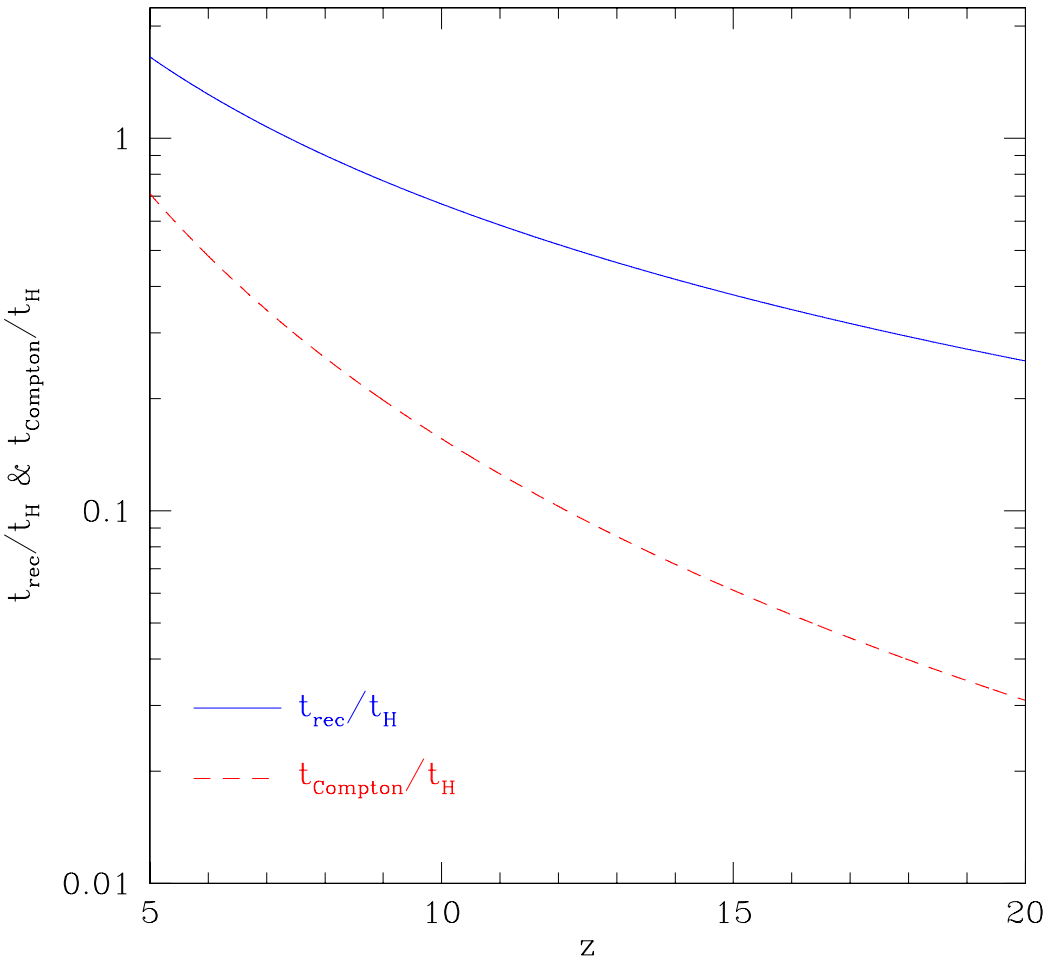

Fig. 10.— shows the ratio of the recombination time to the Hubble time (solid curve) and ratio of the Compton cooling time to the Hubble time (dashed curve) a function of redshift.

with observations (Gnedin 2000a). The value of $f_{\rm es} \times e_{\rm UV}$ is normalized such that the second universal reionization is completed at $z = 6$, as observed. We note that it is possible to vary the values of these three parameters but the results do not alter significantly within plausible ranges.

We see that the universe becomes opaque to Lyα photons very quickly following the first reionization at $z = 17$, since a very small amount of neutral hydrogen suffices to blank out all Lyα emission, and it remains opaque until $z = 6$. However, hydrogen is significantly ionized with $n_{\rm HII}/n_{\rm H} \geq 0.4$ throughout the long second reionization process. To better understand this rather complicated reionization process we plot in Figures (7,8,9) the evolution of temperature, clumping factor and stellar fraction, respectively, as a function of redshift. In addition, in Figure 10, we show the ratio of hydrogen recombination time over the Hubble time and the ratio of Compton cooling time over the Hubble time. It is noted that at the redshift and density of interest Compton cooling dominates over other cooling terms.

From Figure 10 we immediately see that the hydrogen recombination time is significantly longer than the Compton cooling time, both of which are shorter than the Hubble time at $z \geq 8$. Therefore, the IGM heated up by the photoionization during the first reionization at $z = 17$ would subsequently cool down more rapidly than recombining, resulting in overcooled but significantly ionized IGM, in the absence of subsequent photoheating. However, substantial cooling reduces the Jeans mass of the IGM and would increase the star formation rate, which would then provide countervailing heating by photoionization. Thus, the temperature of the IGM may be somewhat self-regulated due to the competition between the Compton cooling and photoheating. For a reasonable cold dark matter based cosmological model such as the one adopted here it happens that the star formation activities are at a level such that the two balancing terms are comparable in magnitude, resulting in a fairly mild evolution of the IGM temperature seen in Figure 7. The initial drop of the IGM temperature from $z = 17$ to $z \sim 13$ indicates that the Compton cooling dominates at the early stage. From $z \sim 13$, photoheating overtakes Compton cooling (plus adiabatic cooling) due to the combined effect that Compton cooling rate decreases rapidly with time [$\propto (1 + z)^4$] and that the fraction of gas formed into stars increases thanks to the increase of density fluctuations and nonlinear mass scale (see Figure 9). With increased star formation rate, more and more gas is ionized and by $z = 6$ the star formation rate surpasses the recombination rate and the universe is reionized. We find that by $z = 6$ about 1.5% of all gas collapsed into Pop II stars and about four photons per baryon have been produced since $z = 17$.

Figure 7 indicates that the mean temperature of the IGM is maintained at $5\times10^3-10^4$K during the entire second reionization process. From Equation (19) we find that for $T = 5 \times 10^3$K, $M_J \sim 6 \times 10^8$ at $z = 13$, which corresponds to halos with virial temperature well

above 8000K (see Figure 4). Thus, in retrospect, star formation activity in halos assisted by hydrogen molecular cooling is negligibly small and most of the star formation occurs in halos where hydrogen atomic line cooling dominates. The earlier assumption that H_2 cooling is sufficient in small halos thus turns out to be unnecessary, while it is still true that star formation in low mass halos could occur by H_2 cooling, *if gas can somehow be collected in them*. The overall gas clumping factor shown in Figure 8 is in reasonable agreement with numerical simulations (Gnedin & Ostriker 1997).

In summary, the second reionization process has several characteristic properties. First, the IGM is maintained "warm" with a temperature of $5 \times 10^3 - 10^4$ K during this second "dark age". Second, the IGM is kept at a significantly ionized state throughout the second reionization period. Finally, the overwhelming fraction of star formation activity responsible for producing the ionizing photons in this period are in halos where atomic line cooling is the primary cooling process.

5. Discussion

The possible indication of a more top-heavy initial stellar mass function (IMF) in early galaxies or earlier stages of galaxies than present-day IMF (Salpeter 1955) was suggested five decades ago (Schwarzschild & Spitzer 1953). Cosmological consequences of the first generation, massive stars at high redshift have been discussed in a variety of contexts (e.g., Layzer & Hively 1973; Carr 1977; Rees 1978; Rowan-Robinson, Negroponte, & Silk 1979; Puget & Heyvaerts 1980; Tarbet & Rowan-Robinson 1982; Carr, Bond, & Arnett 1984).

The reionization picture presented here would have a wide range of profound implications for many aspects of structure formation. There are many questions that need to be addressed. It is beyond the scope of this paper to explore any of these issues in significant details and we will study these and other relevant issues in subsequent investigations. But we will give some simple estimates or analysis for some selected issues.

5.1. Initial IGM Metal Enrichment

Direct observational evidence for massive Pop III stars may be just emerging recently. While Luck & Bond (1985) and others have previously indicated the need for VMS ($M > 100\,M_\odot$) to explain the overabundant α elements, Qian, Wasserburg and collaborators (Wasserburg & Qian 2000; Qian & Wasserburg 2000,2002; Oh et al. 2001; Qian, Sargent, & Wasserburg 2002) have recently stressed the unique signature of Pop III VMS and suggested that

Pop III stars could promptly produce the observed abundance patterns of metal poor stars (McWilliam et al. 1995; Ryan, Norris, & Beers 1996; Rossi, Beers, & Sneden 1999; Norris, Ryan, & Beers 1997,2001).

Given the shallow potential wells of Pop III galaxies, supernova explosions would likely blow away the ejectas along with a large fraction of the diffuse interstellar gas (Mac Low & Ferrara 1999; Mori, Ferrara & Madau 2002). The predicted fraction of baryonic mass $f_{\rm III} \sim 3.4 \times 10^{-3} c_1^* = 3.4 \times 10^{-5} (c_1^*/0.01)\,{\rm Z}_\odot$, formed into Pop III stars (see Figure 3, using critical virial temperature $T_{\rm v} = 2000$K for minihalos; HAR; GB) would then produce a mean metallicity of $\sim 1.7 \times 10^{-3} \xi_{\rm IMF} (c_1^*/0.01)$ produced by Pop III supernovae. This is in agreement with the observational analyses of Qian & Wasserburg, who note that [Fe/H]=-3 marks the transition; at lower value VMS dominates the enrichment, whereas at higher value a sharp rise in the abundances of the heavy r-process elements such as Ba and Eu in galactic halo stars with [Fe/H]≥ -3 signifies the occurrence of Type II supernovae of normal stars with masses of $10 - 60\,{\rm M}_\odot$. One may expect to see the Pop III star abundance patterns in low density regions of the universe, such as Lyα clouds or voids, where subsequent additional enrichment may be minute.

5.2. Intergalactic Magnetic Field

Another possible consequence of supernova explosion and expulsion of the gas into the IGM is the magnetic feedback to the IGM. Let us give a simple estimate here. We should use local observations as a guide. The Crab Nebula (a plerion) has a magnetic field of strength $B \sim 100\mu$G currently occupying a sphere of radius $r \sim 1$ pc, totaling a flux of $\psi_{\rm Crab} \sim 3 \times 10^{33}$ G cm^2. Assuming flux conservation and Pop III magnetic bubble filling factor of unity give $B_{\rm IGM} = (\frac{f_{\rm III}\rho_b(1+z_{\rm ej})^3}{M_{\rm III}})^{2/3} (\frac{M_{\rm III}}{M_{\rm Crab}}) \psi_{\rm Crab}$, where $M_{\rm III} \sim 100\,{\rm M}_\odot$ is the mass of a typical Pop III star, $M_{\rm Crab} \sim 5\,{\rm M}_\odot$ is the zero-age main sequence progenitor star for Crab; $f_{\rm III} \sim 3.4 \times 10^{-5}$ is the fraction of baryons formed into Pop III stars (see Figure 3); ρ_b is the mean baryonic density at zero redshift; $z_{\rm ej}$ is the redshift of ejection of the magnetic field into the IGM; we have assumed that the magnetic flux is approximately proportional to the stellar mass. Inserting all the numbers gives $B_{\rm IGM}(z = 17) \sim 3 \times 10^{-10}$ G at $z = 17$ and subsequently $B_{\rm IGM}(z) \sim 3 \times 10^{-10} (\frac{1+z}{18})^2$ G. This magnetic field, seemingly having a significantly larger amplitude than that produced by gravitational shocks in the collapse of large-scale structure (Kulsrud et al. 1997), could serve as a seed field for subsequent galaxy formation. The mean separation between Pop III galaxies of mass $10^5 - 10^6\,{\rm M}_\odot$ with a mass fraction of $10^{-2.5}$ is $\sim 50 - 100$ comoving kpc. Thus, if Pop III supernovae are responsible for enriching the IGM relatively uniformly to a metallicity of about a thousandth of the solar

value, it is also likely that the magnetic field lines originating from supernovae remnants would be stretched to fill up the intergalactic space, resulting in an initial magnetic field possibly coherent on scales as large as $50 - 100$kpc.

In addition, miniquasars powered by Pop III black holes may produce mini radio jets, supported by the observational fact that radio jets are observed in accretion disks on a wide range of scales in a wide variety of astrophysical systems. The magnetic field from miniquasars may be as important as or more important than that from the Pop III stars; but a reliable estimate is difficult.

5.3. Pop III Black Holes

Without fine tuning the IMF of Pop III stars, it seems likely that $\sim 200\,\mathrm{M}_\odot$ black hole from Pop III stars more massive than $260\,\mathrm{M}_\odot$ and smaller black holes ($M_{\rm BH} \sim 10 - 50\,\mathrm{M}_\odot$) from Pop III stars less massive than $140\,\mathrm{M}_\odot$ would form. The possible bimodality of the distribution of black hole mass is interesting but the consequences are too complicated to be easily outlined. But those black holes will be building blocks for formation of subsequent structures and the question is: where will they go? In general, since there is no correlation between the small-scale structures that form Pop III galaxies and later structures, one would expect to find those black holes in all environments, including globular clusters, galaxy halos and intergalactic space. It is possible that the dynamic formation of halos and galaxies in hierarchical structure formation may be significantly altered in the presence of these massive black holes, especially in the cores of the relevant structures, such as globular clusters, galaxies, etc. The number density of Pop III black holes of mass $\sim 100\,\mathrm{M}_\odot$ is of order $(100 - 1000)(c_1^*/0.01)$ per comoving Mpc^3, comparable to the number density of globular clusters. It is quite possible that many globular clusters could be seeded by those black holes. Finally, the Pop III black holes are clearly more than abundant enough to provide seeds for later supermassive black holes seen in centers of local galaxies (e.g., Tremaine et al. 2002), AGN and quasars (e.g., Rees 1984,1990).

5.4. Pop III Hypernovae as Gamma-Ray Bursts

Could the supernovae or hypernovae of Pop III stars be some of the observed gamma-ray bursts (GRBs) (e.g., Cen 1998,1999; Hoeflich, Wheeler, & Wang 1999; Paczynski 1998,2001; Wheeler et al. 2000)? If the association of supernovae-GRBs at lower redshift where observations are able to attain is a guide (e.g., Dado, Dar & De Rujula 2002), one may naturally

expect that the more massive counterparts (hypernovae) of Pop III stars should produce similar but perhaps (intrinsically) more energetic GRBs. Since this may be an indirect but important way to detect Pop III stars, we will make a more quantitative analysis.

We will adopt the standard fireball external shock model for GRBs (Rees & Meszaros 1992). In this case, the overall duration of a GRB would scale as

$$\Delta t_{\rm GRB,obs} \propto \frac{E^{1/3}}{\Gamma^{8/3}} \frac{1+z}{n_{\rm ISM}^{1/3}} \propto \frac{E^{1/3}}{\Gamma^{8/3}} \propto E^{-7/3}, \tag{22}$$

where E is the fireball energy per unit solid angle; Γ is the terminal Lorentz factor of the fireball (or firecone or the like); $n_{\rm ISM}$ is the interstellar density into which the fireball propagates; z is redshift. The term $(1+z)$ takes into account cosmological time dilation. We have argued that $n_{\rm ISM} \propto (1+z)^3$, resulting in the second proportionality in Equation (22). In the absence of reliable knowledge how E relates to Γ, we assume that GRBs have the same baryon load thus $E \propto \Gamma$, yielding the third proportionality in Equation (22). The energy of Pop III hypernovae is assumed to be approximately a factor 7 larger than the low redshift normal supernovae that produce low redshift GRBs and we hence assume that the fireball energy per unit solid angle for Pop III hypernovae, $E_{\rm GRB,III}$, is a factor of 7 larger than the low redshift counterpart, $E_{\rm GRB,normal}$. Under these simple assumptions we arrive at the conclusion that GRBs due to Pop III stars at high redshift have observed durations about a factor of 100 shorter than low redshift GRBs. We conjecture that this shorter duration GRBs may correspond to the observed subset of GRBs peaked at $T_{90} \sim 0.2$ sec, whereas the lower redshift counterparts correspond to those peaked at $T_{90} \sim 20$ sec (Mazets et al. 1981; Norris et al. 1984; Kouveliotou et al. 1993). There is, however, some supportive evidence for this conjecture.

First, let us estimate the expected flux in the gamma-ray. The gamma-ray flux is

$$F_\gamma \propto \frac{E/\Delta t_{\rm GRB,obs}(1+z)}{d_L^2} \propto E^{10/3} d_{\rm cm}^{-2} (1+z)^{-3}, \tag{23}$$

where the term $(1+z)$ in the first proportionality is to factor back the cosmological dilation term in the observed GRB duration (Equation 22); luminosity distance is $d_L = d_{\rm cm}(1+z)^2$, where $d_{\rm cm}$ is the comoving distance. If we use redshift for Pop III GRBs $z_{\rm III} = 17$, for normal GRBs $z_{\rm normal} = 1.5$, $E_{\rm GRB,III}/E_{\rm GRB,normal} = 7$, $d_{\rm cm,III}/d_{\rm cm,normal} = 2.5$ (for the adopted cosmological model), we obtain $F_{\rm III,\gamma}/F_{\rm normal,\gamma} = 0.29$, which is in good agreement with observations (Paciesas et al. 1999).

Second, the observed GRB photon energy (frequency) is $\nu_{\rm obs} = \Gamma \nu_{in} (1+z)^{-1}$, where Γ is Doppler shift and $(1+z)$ is red shift. The intrinsic frequency of photons in the restframe, ν_{in}, depends on many factors including electron energy distribution and magnetic field in

the fireball frame; we have no *a priori* reason to argue that the electron energy distribution and magnetic field in the Pop III GRBs should parallel those of the low redshift GRBs. It is, however, highly likely that Pop III hypernovae, having higher energy and higher Lorentz factor, and propagating into denser gas, should have more emitted photons at higher intrinsic frequencies. Consequently, we should expect that the observed Pop III GRBs should have harder spectra than the low redshift GRBs, consistent with observations (Kouveliotou et al. 1983) [note that $\Gamma(1+z)^{-1}$ is about the same for both high and low redshift GRBs].

Third, for the afterglow, the characteristic (peak) time in observer's frame for emission at observed frequency ν scales as $t \propto \nu^{-2/3}$ (in the simplest model where magnetic field energy density in the postshock region is assumed to be a fixed fraction of the total energy density and the typical electron energy density is also assumed to be proportional to the total energy density). Thus, for the Pop III GRBs in our model we expect to see peak flux at $(2\mathrm{keV}, 2\mathrm{eV}, 8\mathrm{GHz})$ at approximately $(2\ \mathrm{sec}, 200\ \mathrm{sec}, 4\ \mathrm{hr})$ after the GRB burst. The afterglow peak fluxes at various frequencies are expected to be comparable to those of the longer duration GRBs at low redshift. For Pop III GRBs at redshift $z = 17$, restframe photons with energy from 10.2 eV (Lyα 1216$\mathring{A}$) to about 1keV will be completely absorbed by intervening neutral IGM. This translates to an observed blockout window from about $2.2\mu m$ to 0.05keV. So far, GRB afterglows have been detected exclusively for long duration GRBs; no afterglow out of four well localized short GRBs has been detected (Hurley et al. 2002). In our model it should not be surprising at all that no optical afterglows have been observed for short duration GRBs, even with relatively rapid follow-ups (about 1000 sec after the burst; Kehoe et al. 2001). The afterglows of the short duration GRBs may be detected at $(2.2\ \mu m, 8\ \mu m, 8\ \mathrm{GHz}, 1\ \mathrm{GHz})$ at $(500\mathrm{sec}, 1000\mathrm{sec}, 4\mathrm{hr}, 15\mathrm{hr})$ after the burst. In the X-ray band a very quick follow-up may be able to detect the afterglow of short GRBs: the X-ray flux drops to about $10^{-13}\mathrm{erg/cm^2/sec}$ one hour after the burst. A follow-up in the infrared may be only done by IRAC on SIRTF, if such quick pointings are possible. Probably the best hope to detect the afterglows of short GRBs is in the radio, although a rapid follow-up (a hour or so after the burst) is required at a flux level of $\sim$ 1mJy. A detection of afterglows at these shorter time scales, compared to the normal, low redshift counterparts, will be a strong test of the proposed model. In the event that afterglows for the short GRBs are detected, our model predicts that their host galaxies would still be too faint to be detectable in the foreseeable future, unless they are magnified by gravitational lensing by an extremely large factor (see §5.5). We note that, although the assumption that $\Gamma \propto E$ made above is rather arbitrary, the characteristics concerning the afterglows are basically scaled from the parent GRB bursts and therefore do not depend on the assumption.

5.5. Detecting Pop III Hypernovae

The total number of Pop III hypernovae (HN) is $N_{\rm HN} = 3.4 \times 10^{-5} \rho_b (4\pi/3) R_{\rm H}^3 / M_{\rm III} = 1.7 \times 10^{15}$, where $M_{\rm III} = 100\,{\rm M}_\odot$ for Pop III star mass is used, $R_H = 6000 h^{-1}$ Mpc is the comoving Hubble radius and ρ_b is the comoving mean baryonic density. We can estimate the Pop III hypernova surface number density at any given time to be

$$\Sigma_{\rm HN} = 1.7 \times 10^{15} \times \left(\frac{\Delta t_{\rm HN}(1+z)}{t_{\rm H}}\right) \left(\frac{1}{4\pi \times 1.2 \times 10^7 {\rm arcmin}^2}\right) \approx 0.85 \text{ arcmin}^{-2}, \quad (24)$$

where $\Delta t_{\rm HN}$ is the time duration of each hypernova event in the hypernova restframe and $t_{\rm H}$ is the age of universe at $z = 17$; the first parenthesized term in the above equation takes account the finite duration of each supernova event and an intrinsic duration for the hypernovae $\Delta t_{\rm HN} = 1$ yr is used; Since Pop III hypernovae may be the only direct probe in the search for Pop III stars [Pop III galaxies are probably too faint to detect even with the James Webb Space Telescope (Stockman & Mather 2000; JWST)], a careful consideration is desirable.

We will examine if the first generation galaxies and their associated hypernovae are directly detectable with SIRTF. The physical sizes of the galaxies in the redshift range $z = 15 - 25$ is unknown but it is perhaps unlikely that they will be larger than their lower redshift counterparts. Steidel et al. (1996) find that the great majority of $z > 3$ objects have a half-light radius ~ 2 kpc, which, if placed at $z_S = 17$, would subtend $\sim 0''.05$ (for the adopted model), more than a factor of ~ 10 below the angular resolution of SIRTF. In other words, these high redshift galaxies are point sources to SIRTF. The flux density (the power per unit antenna area and per unit frequency interval) of a point source (without cosmological surface brightness dimming) at frequency ν is (Weinberg 1972):

$$S = \frac{P(\nu[1+z_{\rm S}])}{(1+z_{\rm S})^3 d_{\rm cm}^2}, \quad (25)$$

where z_S is the source redshift and ν is the observed photon frequency. P is the intrinsic power, the power emitted per unit solid angle and per unit frequency interval, related to the luminosity L of the source by $P = L/4\pi\Delta\nu$, where $\Delta\nu$ is the rest frame bandwidth at which the source has a luminosity L; $d_{\rm cm}$ is the comoving distance to the source. Using a rest frame band $0.09 - 0.27 \mu m$ (corresponding to the observer's band $1.6 - 4.8\ \mu m$) and $z_{\rm S} = 17$ we obtain

$$S = 0.67 (\frac{L}{10^9 L_\odot}) \text{ nJy}. \quad (26)$$

The point source detection sensitivity at 1σ level (for relatively long integration time $>$ 500 seconds) of the Infrared Array Camera (IRAC) on SIRTF at $3.5 - 4.5\ \mu m$ is (SIRTF

Project 1997) $S_{3.5} \approx \sqrt{(100/t) + 0.6^2}$ μJy, where t is the integration time in seconds. The second term inside the square root is the confusion noise limit due to faint unresolved sources, modeled by Franceschini et al. (1991). The total luminosity of a Pop III galaxy is $L = 5 \times 10^7 (c_1^*/0.01)(M_{\rm h}/10^6\,{\rm M}_\odot)\,{\rm L}_\odot$; only a small fraction of the total luminosity is in the indicated band. It is clear that no Pop III galaxies will be detectable by SIRFT, even without the confusion noise limit.

The situation for the associated Pop III hypernovae is significantly improved, due to the higher luminosity and nature of their time variability. It we assume that the optical luminosity of the hypernovae to be 1×10^{10} $L_\odot$ (about 10 times that of the local normal supernovae), the flux density of Pop hypernovae will be at a level $\sim 0.01\mu$Jy. Even without background confusion (*if the variable source has a variability time scale shorter than the indicated integration time*), in order to detect such a flux density at 1σ level, an integration time of 11 days on IRAC will be required, which seems impractical. Even if this long integration is achievable, the fact that the variability time scale of a hypernovae at the considered redshift may be quite long indicates that it will be extremely difficult to directly detect high redshift hypernovae, *unless their flux is significantly amplified*.

In Appendix A we derive the probability of strong gravitational lensing by massive clusters of galaxies and find that a random source behind a massive galaxy cluster will have a probability

$$P_{\rm clust}(\mu) = \frac{6.7 \times 10^{-2}}{\mu^2} \left(\frac{\Omega_{\rm FOV}}{25\ {\rm arcmin}^2} \right)^{-1} \tag{27}$$

being magnified by $\geq \mu$, where μ is the lensing magnification and $\Omega_{\rm FOV}$ is the field of view of a telescope. The number of Pop III hypernovae, magnified by $\geq \mu$, per field of view centered on a massive cluster is then

$$N_{HN} = P_{\rm clust}(\mu)\Omega_{\rm FOV}\Sigma_{\rm HN}. \tag{28}$$

In order for the IRAC camera of SIRTF to detect at $n\sigma$ statistical level a point source, which would have a flux density of S in the absence of gravitational lensing magnification, one requires that

$$S\mu = n\sqrt{100/t}, \tag{29}$$

where point source confusion limit is removed; t is integration time in seconds. We plot the number of hypernovae, $N_{\rm HN,det}$, per field of view detected at 3σ confidence level against integration time t in Figure 11, assuming $L_{\rm HN} = 1 \times 10^{10}\,{\rm L}_\odot$ giving unlensed flux density of $S = 6.7$nJy at the observed wavelength of several μm. To put the matter in perspective, 1,000 target fields each with 10k-second integration time would detect ~ 100 multiply lensed Pop III hypernovae at 3σ confidence level.

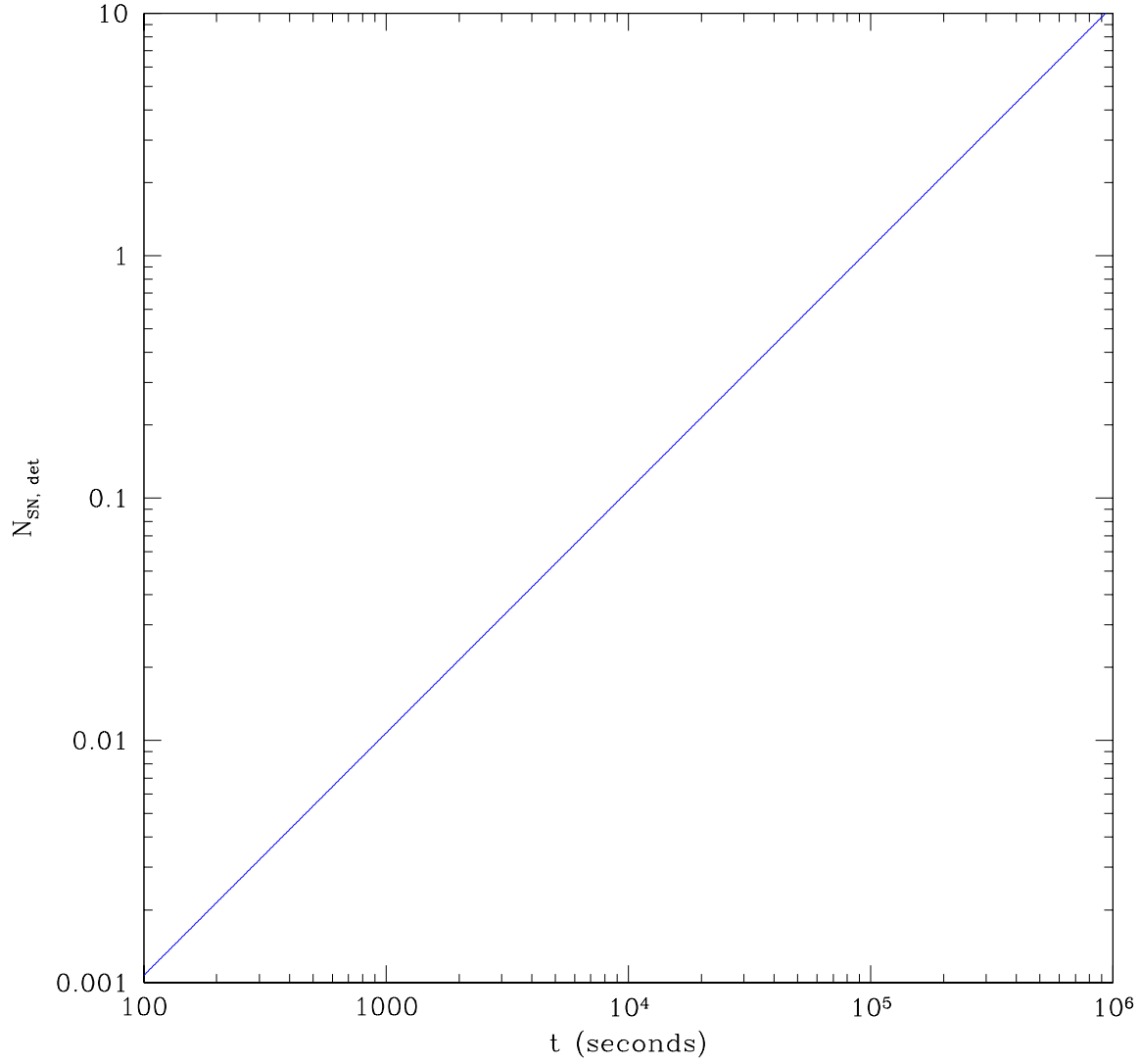

Fig. 11.— shows the average number of strong gravitational lensing magnified Pop hypernovae that will be observed per IRAC field of view (25 arcmin^2) as a function of integration time.

We note that since only highly magnified Pop III hypernovae will be observable, the observed candidates should have distinct features: the multiple images will significantly help the identification process. If the cluster lens is known, its lens potential derived independently elsewhere would further constrain the image configurations. Once such images are found, periodic monitoring up to a few years would eventually verify the transient nature of the Pop III hypernovae. Since the total number of detectable hypernovae is just proportional to the total integration time, one could choose an optimal strategy such that the observation is most sensitive to the expected splittings of the images: a shorter exposure will require a higher magnification from a more central region of the lens, where splittings may decrease due to a smaller velocity dispersion at the center of the cluster.

5.6. Effects on the Cosmic Microwave Background

The earlier reionization at $z = 17$ would significantly increase the electron Thomson scattering optical depth. This is so because the IGM ionization fraction remains appreciable during the period between the first reionization ($z = 17$) and the second reionization ($z = 6.1$), even though the IGM temperature has dropped to a few thousand Kelvin due primarily to Compton cooling by the cosmic microwave background (CMB). Figure 12 shows the cumulative Thomson scattering optical depth as a function of redshift. We see that the Thomson scattering optical depth increases from $\tau_e(z < 6.1) = 0.027$ to $\tau_e(z < 17) = 0.079$. Evidently, the first reionization boosts the optical depth of the second reionization by a factor of ~ 3, making the total Thomson optical depth much more significant. The implications for the CMB, in particular, for polarization of the CMB, will be significant. We will not attempt to make further detailed analysis here but refer readers to the vast amount of literature available on the subject; for an excellent recent review see Hu & Dodelson (2002).

5.7. Non-detection of Pop III Stars Locally

There is a long history of search for Pop III stars (Bond 1970,1981; Hills 1982; Bessell & Norris 1984,1987; Carr 1987; Cayrel 1996) or primeval galaxies (Partridge 1974; Davis & Wilkinson 1974). If Pop III stars are as massive as suggested, perhaps it is not surprising that no single Pop III star should have been found, while over 100 metal-poor stars with $-4 < [Fe/H] < -3$ have been found (Cayrel 1996), since all Pop III stars would end either as supernovae or black holes. The proposed model, unfortunately, would mark the end of search for Pop III stars in the local universe.

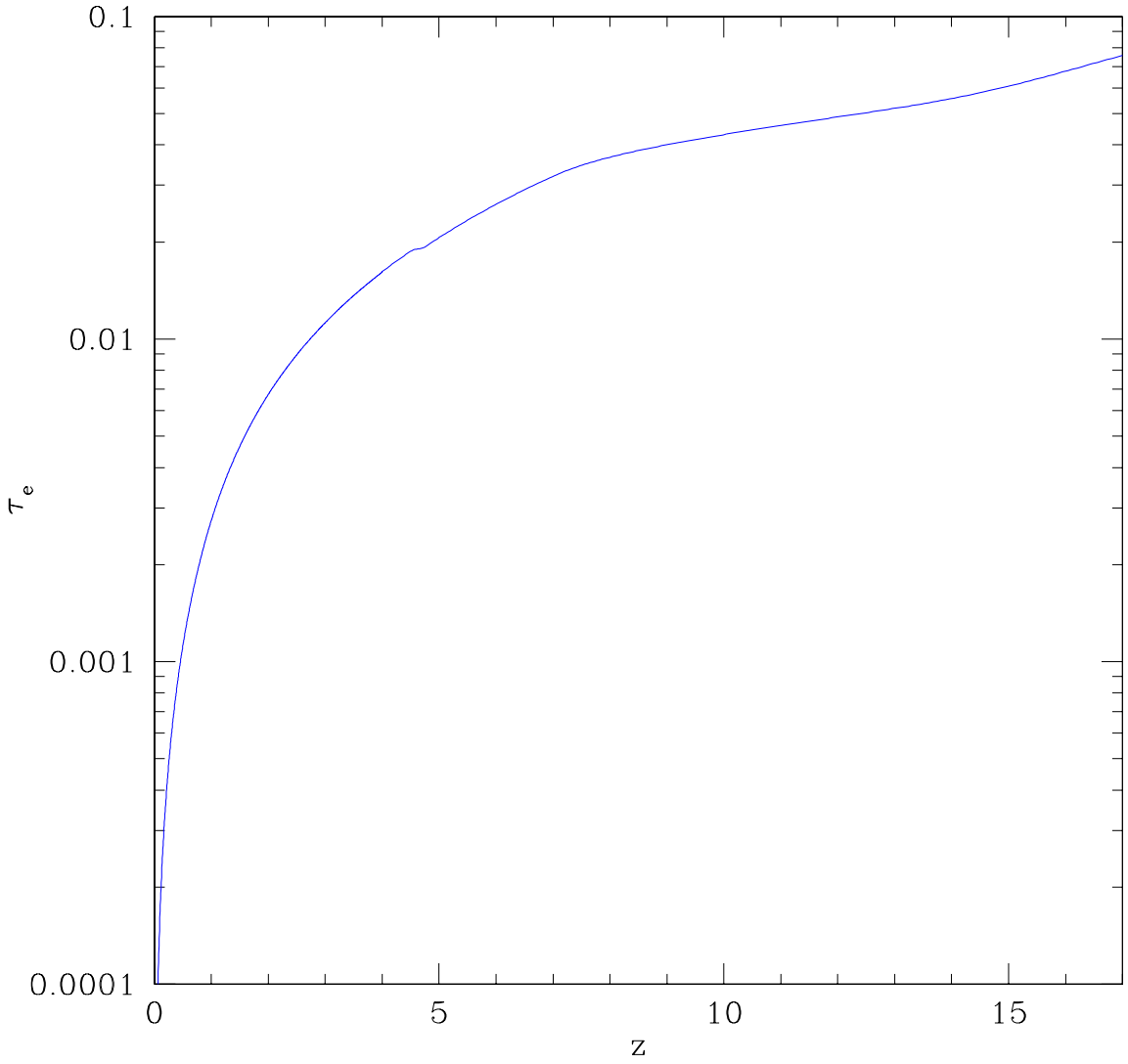

Fig. 12.— shows the cumulative Thomson scattering optical depth as a function of redshift.

5.8. Detectability of Galaxies Beyond $z = 6$

It is interesting to note, from Figure 6, that there is a substantial redshift range beyond the end redshift of the reionization $z = 6$, where the IGM is already substantially ionized. For example, $n_{HI}/n_H \sim 0.01$ at $z \sim 6.5$ and $n_{HI}/n_H \sim 0.03$ at $z \sim 7.0$. This feature of an extended redshift interval of high ionization appears to be generic in all variant models with different combination of $C_{\rm halo}$ and $f_{\rm es} \times e_{\rm UV}$. This result would have interesting consequences on the observability of galaxies beyond the second reionization epoch. Taking the result at face value, for a galaxy at $z = 6.5$, the Strömgren sphere produced by the galaxy would be a factor of about 5 larger than that with the case where the galaxy is embedded in a completely neutral IGM. This would reconcile the seemingly conflicting observational claims: on one hand, the universe appears to be reionized at $z \sim 6$ when ionizing radiation background is seen to rise sharply (e.g., Fan et al. 2001; Becker et al. 2001, Barkana 2001; Cen & McDonald 2002); on the other hand, Lyα galaxies at redshift as high as $z = 6.56$ (Hu et al. 2002) has been detected. In the model presented here the Strömgren sphere for this Lyα galaxies at $z = 6.56$ will be large enough (with a radius of order a megaparsec proper), which, combined with a much lower neutral fraction in the IGM, would enable the Lyα line be transmitted without substantial absorption (Miralda-Escude & Rees 1998; Cen & Haiman 2000; Madau & Rees 2000). One prediction is that the number of observable Lyα galaxies would drop sharply beyond $z \sim 7$.

5.9. Hydrogen 21cm Absorption by Minihalos Prior to the Second Cosmological Reionization: A Test

The mean, neutral medium expanding with the Hubble flow at redshift z would produce an optical depth for the hydrogen 21 cm resonant absorption is (Shklovsky 1960)

$$\bar{\tau}(z) = \frac{n(z)}{H(z)} \frac{g_2}{g_1(g_2+g_1)} A_{21} \frac{c^3}{8\pi\nu^3} \frac{h\nu}{kT_{\rm sp}} = 8.5 \times 10^{-4} (\frac{T_{\rm sp}}{200{\rm K}})^{-1} (\frac{\Omega_{\rm b}h^2}{0.02}) (\frac{\Omega_{\rm M}h^2}{0.15})^{-1/2} (\frac{1+z}{8})^{3/2} \tag{30}$$

where $H(z)$ is the Hubble constant at redshift z; $n(z)$ is the mean atomic hydrogen number density at z; $g_1 = 1$ and $g_2 = 3$ are the statistical weights of the lower and upper hyperfine levels; ν is the frequency of the hydrogen 21cm line; $T_{\rm sp}$ is the spin temperature of the atomic hydrogen; ν is the frequency of the 21 cm line; c is the speed of light; k is the Boltzmann's constant; A_{21} is the spontaneous decay rate of the hyperfine transition of atomic hydrogen; Ω_M and Ω_b are total matter and baryonic matter density at $z = 0$ in units of closure density; $h = H_0/100$km/s/Mpc, where H_0 is the Hubble constant at $z = 0$. Clearly, the uniform medium would only cause a very modest absorption at redshift $z \sim 6 - 17$.

Minihalos would cast significantly larger optical depth. For 21cm absorption by atomic hydrogen in virialized minihalos we may rewrite Equation (30) approximately as:

$$\tau_h(z) = \frac{178 n(z) r_v}{\sigma_v} \frac{g_2}{g_1(g_2+g_1)} A_{21} \frac{c^3}{8\pi\nu^3} \frac{h\nu}{kT_{\rm sp}} \tag{31}$$

where r_v and σ_v are the virial radius and velocity dispersion within the virial radius, respectively; the factor 178 is the relative overdensity of matter within the virial radius. Using relations $\sigma_v = GM_v/2r_v$, $M_v = 178(4\pi/3)\rho(z)r_v^3$ [where $\rho(z)$ is the mean total density at z] and the definition of Hubble constant, we can transform Equation (31) to

$$\tau_h(z) = 2\sqrt{178}\bar{\tau}(z) = 0.023 (\frac{T_{\rm sp}}{200{\rm K}})^{-1} (\frac{\Omega_b h^2}{0.02}) (\frac{\Omega_M h^2}{0.15})^{-1/2} (\frac{1+z}{8})^{3/2}. \tag{32}$$

We see that gaseous minihalos with $T_{\rm sp} \sim 10^2 - 10^3$, *if they exist*, could produce significant optical depths at 21 cm at a level of $0.01 - 0.1$ (Furlanetto & Loeb 2002; see also Carilli, Gnedin & Owen 2002 for a numerical treatment). Note that the spin temperature $T_{\rm sp}$ would be bracketed by the cosmic microwave background temperature and the kinetic temperature (approximately the virial temperature) of a minihalo.

Furlanetto & Loeb (2002) have pointed out that the 21 cm forest produced by minihalos prior to cosmological reionization will be detectable by the next generation of low-frequency radio telescopes, such as Low Frequency Array (LOFAR) and Square Kilometer Array (SKA). However, this will only be possible, *if the minihalos could retain their gas*, as they would in the conventional reionization scenario. In the reionization scenario presented here, all gas was driven out of minihalos by either internal photoheating, or external photoheating at the first reionization at $z \sim 15 - 20$ or supernova explosions, and the gas was never able to return to minihalos due to the sustained high temperature of the IGM ($T_{\rm IGM} \geq 5 \times 10^3$K; IGM at this temperature corresponds to a Jeans mass of $\sim 10^9\,{\rm M}_\odot$) throughout the second reionization period. Consequently, in our scenario, 21 cm forest lines, which would otherwise be produced by minihalos without the first reionization, have all been wiped out. This will be a definitive test to distinguish between the two scenarios.

5.10. Uncertainties

Perhaps the most uncertain in the chain of derivation is the IMF of the Pop III stars. However, most of the main conclusions, including positive feedback of Pop III star formation and two times of cosmological reionization, are likely to hold for any sufficiently top-heavy IMF. While the simulations with sub-solar mass resolution (Abel et al. 2002; Bromm et al.

2002) have clearly shown the formation of Pop III VMS, it is yet unclear what the angular momentum transport mechanisms are. It is possible, in principle, that hydrodynamic processes, included in the quoted simulations, could transport the unwanted angular momentum outward, as the simulators have advocated. If local star formation is a guide, one could imagine that very massive Pop III stars may form in binaries or multiples, in which case angular momentum removal would be easily achieved. It is also intriguing to note that, if we extrapolate the observed ratio of super massive black hole to bulge mass (e.g., Tremaine et al. 2002), then one would expect to find a black hole of mass $\sim 100 - 1000\,\mathrm{M}_\odot$ at the center of each minihalo of mass $10^5 - 10^6\,\mathrm{M}_\odot$. Thus, perhaps one should not be too surprised that nature has managed to form a compact object (star) of mass $\sim 100\,\mathrm{M}_\odot$ formed at the center of a minihalo, if the quoted observations are any empirical guide; it may be argued, angular momentum-wise, that it is a less stringent task to collapse a higher density gas cloud at higher redshift to form a star than a lower density gas cloud at lower redshift to form a black hole, as observed.

We have ignored the possible contribution from quasars to the second reionization process. If the emission rate of ionizing photons from quasars is proportional to the star formation rate, as indicated by low redshift observations (Boyle & Terlevich 1998; Cavaliere & Vittorini 1998), then, to zero-th order, all that is needed is to renormalize $f_{\rm es} \times e_{\rm UV}$ such that the second reionization completes at $z \sim 6$ and results would, to zero-th order, remain unchanged.

6. Conclusions

We have shown that Pop III stars can continue to form under the positive feedback effect of X-ray emission produced by the cooling energy of supernova blast waves of exploding Pop III stars and miniquasars powered by Pop III black holes. As a result, Pop III stars can, for the first time, reionize and heat the universe at $z \sim 15 - 20$, contrary to the conventional expectation. However, the ionized state of the universe cannot be maintained due to rapid recombination and diminished star formation rate subsequent to the first reionization because of a dramatic increase in Jeans mass. The universe quickly becomes opaque again to Lyα and ionizing photons, marking the second cosmological recombination. The subsequent evolution of the IGM is complicated and shows a prolonged process for reionizing the universe for the second time from $z \sim 15 - 20$ up to redshift $z \sim 6$. The ionizing sources for the second reionization are, however, not limited to stars in halos with virial temperature above 10^4 K, although in practice most of the star formation activities occur in halos dominated by atomic hydrogen line cooling due to the high Jeans mass of the IGM. Compton cooling by the cosmic

microwave background and photoheating by the stars self-regulate the Jeans mass and the star formation rate. The mean temperature of the intergalactic medium is maintained at $5 \times 10^3 - 10^4$ K from $z = 15 - 20$ to $z = 6$. Photoionization and recombination also balance one another such that the mean ionization fraction of the intergalactic medium is kept in a rather narrow range $n_{\rm HII}/n_{\rm H} \sim 0.4 - 1.0$ from $z = 15 - 20$ to $z = 6$. The end of the second reionization has been witnessed by the latest observations of high redshift quasars (e.g., Fan et al. 2001; Becker et al. 2001, Barkana 2001; Cen & McDonald 2002). But the first reionization as well as its ionizing sources would require future missions such as SIRTF and JWST to detect. The complex process of the second reionization requires more detailed study and the possibility of probing this long process needs to be quantified more rigorously using detailed simulations with 3-d radiative transfer.

There is a wide range of interesting implications from this new reionization picture presented here. To highlight a few:

• The Pop III stars enrich the IGM with a metallicity of $\sim 10^{-3}\,{\rm Z}_\odot$ at $z \sim 15 - 20$ with a distinct abundance pattern.

• The magnetic field originating from massive stars could pollute the IGM with a large-scale coherent field ($l \sim 50 - 100$kpc) of order $\sim 10^{-10}$ G at $z \sim 15 - 20$.

• The number density of Pop III massive black holes ($10 - 300\,{\rm M}_\odot$) is comparable to that of globular clusters and could seed later structure formation.

• Pop III hypernovae/supernovae may constitute a significant portion of short duration gamma-ray bursts ($t_{90} \sim 0.2$ s), with a number of characteristics consistent with extant observations of GRBs and a number of tests that may be made to verify this proposal.

• Direct detection of Pop III hypernovae/supernovae are very difficult but a systematic search for gravitational lensing magnified Pop III hypernovae/supernovae targeted at massive clusters of galaxies may turn out to be fruitful; SIRTF may be able to detect them.

• The Thomson scattering optical depth is increased to 0.08 from 0.027 due to the first reionization, which may have significant implications on the polarization observations of the cosmic microwave background.

• Under the present scenario it would not have been a surprise that no Pop III stars have been found in the local universe.

• The IGM, while opaque to Lyα photons, is highly ionized ($n_{\rm HI}/n_{\rm H} \sim 0.01$) up to redshift $z \sim 7$. This may reconcile the observation indicating the completion of second reionization at $z \sim 6$ with the detection of Lyα galaxies at redshift $z = 6.56$.

• Finally, in contrast to the conventional reionization scenario, 21 cm forest lines prior to $z = 6$, which would otherwise be produced by minihalos in the absence of the first cosmological reionization, are predicted not to exist. This would provide a definitive test of of the scenario.

This research is supported in part by NSF grant AST-0206299.

REFERENCES

Abel, T., Anninos, P., Norman, M.L., & Zhang, Y. 1998, ApJ, 508, 518

Abel, T., Norman, M.L., & Madau, P. 1999, ApJ, 523, 66

Abel, T., Bryan, G.L., & Norman, M.L., 2000, ApJ, 540, 39

Abel, T., Bryan, G.L., & Norman, M.L., 2002, Science, 295, 93

Bahcall, N.A., et al. 2002, astro-ph/0205490

Bahcall, N.A., Fan, X., & Cen, R. 1997, ApJ, 485, L53

Bahcall, N.A., & Cen, R. 1993, Astrophys. Lett., 407, L49

Barkana, R., & Loeb, A. 1999, ApJ, 523, 54

Barkana, R., & Loeb, A. 2000, ApJ, 539, 20

Barkana, R., & Loeb, A. 2001, Phys. Rep., 349, 125

Barkana, R., 2001, astro-ph/0108431

Barnes, J., & Efstathiou, G. 1987, ApJ, 319, 575

Becker, R.H., et al. 2001, astro-ph/0108097

Bessell, M.S., & Norris, J. 1984, ApJ, 285, 622

Bessell, M.S., & Norris, J. 1987, J. Astrophys. Astr., 8, 99

Bertschinger, E. 1986, ApJ, 304, 154

Blandford, R.D, Kochanek, C.S., Kovner, I., & Narayan, R. 1989, Science, 245, 824

Bond, J.R., Arnett, W.D., & Carr, B.J. 1984, ApJ, 280, 825

Bond, H.E. 1970, ApJS, 22, 117

Bond, H.E. 1981, ApJ, 248, 606

Bookbinder J, Cowie, L.L., Krolik, J.H., Ostriker, J.P., & Rees, M. 1980, ApJ, 237, 647

Boyle, B.J., & Terlevich, R.J. 1998, MNRAS, 293, L49

Bromm, V., Coppi, P.S., & Larson, R.B. 1999, ApJ, 527, L5

Bromm, V., Coppi, P.S., & Larson, R.B. 2002, ApJ, 564, 23

Bromm, V., Kudritzki, R.P., & Loeb, A. 2001, ApJ, 552, 464

Bullock, J.S., Dekel, A., Kolatt, T.S., Kravtsov, A.V., Klyping, A.A., Porciani, C., & Primack, J.R. 2001, ApJ, 555, 240

Burke, J.R., & Silk, J. 1974, ApJ, 190, 1

Carilli, C.L., Gnedin, N.Y., & Owen, F. 2002, ApJ, 577, 22

Carlberg, R.G. 1981, MNRAS, 197, 1021

Carr, B.J. 1977, A& A, 60, 13

Carr, B.J., Bond, J.R., & Arnett, 1984, ApJ, 277, 445

Carr, B. 1987, Nature, 326, 829

Cavaliere, A, & Vittorini, V. 1998, in The Young Universe, ed. S. D'Odorico, A. Fontana, & E. Giallongo (Astron. Soc. Pac., San Francisco), p26

Cayrel, R. 1996, Astron. Astrophys. Rev. 7, 217

Cen, R. 1998, ApJ, 507, L131

Cen, R. 1999, ApJ, 524, L51

Cen, R. 2002, ApJS, 141, 211

Cen, R., & Haiman, Z. 2000, ApJ, 542, L75

Cen, R., & McDonald, P. 2002, ApJ, 570, 457

Cen, R., & Ostriker, J.P. 1993, ApJ, 417, 404

Cen, R., Dong, F., Bode, P.W., & Ostriker, J.P. 2002, in preparation

Cen, R., Gott, J.R., III, Ostriker, J. P., & Turner, E.L. 1994a, ApJ, 423, 1

Cen, R., Ostriker, J.P., Prochaska, J.X., Wolfe, A.M. 2001, in preparation

Chevalier, R.A., 1974, ApJ, 188, 501

Chevalier, R.A., 1982, ApJ, 258, 790

Chevalier, R.A., Imamura, J.N. 1982, ApJ, 261, 543

Cioffi, D.F., McKee, C.F., & Bertschiner, E. 1988, ApJ, 334, 252

Cole, S., & Lacey, C. 1996, MNRAS, 281, 716

Cox, D.P. 1972, ApJ, 178, 159

Couchman, H.M.P., & Rees, M.J. 1986, MNRAS, 221, 53

Dado, S., Dar, A., & De Rujula, A. 2002, A& A, 388, 1079

Davis, M., & Wilkinson, D.T. 1974, ApJ, 192, 251

Del Popolo, A. 2001, MNRAS, 325, 1190

Draine, B.T., & McKee, C.F. 1993, ARAA, 31, 373

Draine, B.T., & Salpeter, E.E. 1979, ApJ, 231, 438

Efstathiou, G. 1992, MNRAS, 256, 43

El Eid, M.F., Fricke, K.J., Ober, W.W. 1983, A& A, 119, 54

Elvis, M., Wilkes, B.J., McDowell, J.C., Green, R.F., Bechtold, J., Willner, S.P., Oey, M.S., Polomski, E., & Cutri, R. 1994, ApJS, 95, 1

Falle, S.A.E.G. 1975, MNRAS, 172, 55

Falle, S.A.E.G. 1981, MNRAS, 195, 1011

Fan, X., et al. 2001, astro-ph/0108063

Ferrara, A. 1998, ApJ, 499, L17

Field, G.B., Somerville, W.B., & Dressler, K. 1966, ARAA, 4, 207

Franceschini, A., De Zotti, G., Toffolatti, L., Mazzei, P., &, Denese, L. 1991, A & A Suppl., 89, 285

Fukugita, M., & Kawasaki, M. 1994, MNRAS, 269, 563

Fukugita, M., & Turner, E.L. 1991, MNRAS, 253, 99

Fuller, T.M., & Couchman, H.M.P. 2000, ApJ, 544, 6

Furlanetto, S.R., & Loeb, A. 2002, astro-ph/0206308

Glatzel, W., Fricke, K.J., & El Eid, M.F. 1985, A& A, 149, 413

Glover, S.C.O., & Brand, P.W.J.L. 2002, astro-ph/0205308 (GB)

Gnedin, N.Y. 2000a, ApJ, 535, L75

Gnedin, N.Y. 2000b, ApJ, 535, 530

Gnedin, N.Y., & Abel, T. 2001, NewA, 6, 437

Gnedin, N.Y., & Ostriker, J.P. 1997, ApJ, 486, 581

Gunn, J.E., & Gott, J.R., III 1972, ApJ, 176, 1

Haiman, Z., Abel, T., & Rees, M.J. 2000, ApJ, 534, 11 (HAR)

Haiman, Z., Rees, M.J., & Loeb, A. 1997, ApJ, 476, 458

Hartquist, T.W., & Cameron, A.G.W. 1977, Astrophys. Space. Sci., 48, 145

Heger, A., & Woosley, S.E. 2002, ApJ, 567, 532

Helfand, D.J., & Moran, E.C. 2001, ApJ, 554, 27

Hills, J.G. 1982, ApJ, 258, L67

Hinshaw, G., & Krauss, L.M. 1987, ApJ, 320, 468

Hirasawa, T., Aizu, K., & Taketani, M. 1969, Prog. Th. Phys. 41, 835

Hogan, C., & Layzer, D. 1977, ApJ, 212, 360

Hoeflich, P., Wheeler, J.C., & Wang, L. 1999, ApJ, 521, 179

Hu, W., & Dodelson, S. 2002, ARAA, 40, 171

Hu, E.M., COwie, L.L., McMahon, R.G., Capak, P., Iwamuro, F., Kneib, J.-P., Maihara, T., & Motohara, K. 2002, ApJ, 568, L75

Hui, L., & Gnedin, N. Y. 1997, MNRAS, 292, 27

Hurley, K., et al. 2002, ApJ, 567, 447

Hutchins, J.B. 1976, ApJ, 205, 103

Kehoe, R., et al. 2001, ApJ, 554, L159

Kessel-Deynet, O., & Burkert, A. 2000, MNRAS, 315, 713

Kochanek, C.S. 1995, ApJ, 453, 545

Kouveliotou, C., et al. 1993, ApJ, 413, L101

Kulsrud, R., Cen, R., Ostriker, J.P., & Ryu, D. 1997, ApJ, 480, 481

Larson, R.B. 1986, MNRAS, 218, 409

Larson, R.B. 1995, MNRAS, 272, 213

Larson, R.B. 2000, in Star Formation from Small to the Large Scale, ed. F. Favata, A.A. Kaas, & A. Wilson (Noordwijk: ESA), p13

Lepp, S., & Shull, J.M. 1984, ApJ, 280, 465

Luck, R.E., & Bond, H.E. 1985, ApJ, 292, 559

Mac Low, M.-M., & Ferrara, A. 1999, ApJ, 513, 142

Machacek, M.E., Bryan, B.L., & Abel, T. 2001, ApJ, 548, 509

Madau, P. 2002, astro-ph/0210268

Madau, P., & Rees, M.J. 2000, ApJ, 542, L29

Magorrian, J., et al. 1998, AJ, 115, 2285

Mao, S. 1991, ApJ, 380, 9

Matsuda, T., Sato, H., & Takeda, H. 1969, Prog. Th. Phys., 42, 219

Mazets, E. 1981, Ap& SS, 80, 3

McKee, C.F., & Ostriker, J.P. 1977, ApJ, 218, 148

McWilliam, A., Preston, G.W., Sneden, C., & Searle, L. 1995, AJ, 109, 2757

Miralda-Escudé, J., & Rees, M.J. 1998, ApJ, 497, 21

Moore, B., et al. 1999, MNRAS, 310, 1147

Mori, M., Ferrara, A., & Madau, P. 2002, ApJ, 571, 40

Nakamura, F., & Umemura, M. 1999, ApJ, 515, 239

Nakamura, F., & Umemura, M. 2001, ApJ, 548, 19

Nakamura, F., & Umemura, M. 2002, ApJ, 569, 549

Nakamura, T., Umeda, H., Iwamoto, K., Nomoto, K., Hashimoto, M.-A.,Hix, W.R., & Thielemann, F.-K. 2001, ApJ, 555, 880

Narayan, R., & Grossman, S. 1989, in Gravitational Lenses, ed. J.M. Moran, J.N. Hewitt, & K.-L. Lo (Berlin: Springer-Verlag), 31

Narayan, R., & White, S.D.M. 1988, MNRAS, 231, 97

Navarro, J.F., Frenk, C.S., & White, S.D.M. 1997, ApJ, 490, 493

Norman, M.L., Paschos, P., & Abel, T. 1998, MmSAI, 69, 455

Norris, J.E., Ryan, S.G., & Beers, T.C. 1997, ApJ, 488, 350

Norris, J.E., Ryan, S.G., & Beers, T.C. 2001, ApJ, 561, 1034

Norris, J., Cline, T., Desai, V., & Teegarden, B. 1984, Nature, 308, 434

Ober, W.W., El Eid, M.F., & Fricke, K.J. 1983, A& A, 119, 61

Oh, S.P. 2001, ApJ, 553, 499

Oh, S.P., Nollett, K.M., Madau, P., & Wasserburg 2001, ApJ, 562, L1

Omukai, K., & Nishi, R. 1998, ApJ, 508, 141

Ostriker, J.P., & Cowie, L.L. 1981, ApJ, 243, L127

Ostriker, J.P., & Gnedin, N.Y. 1996, ApJ, 472, L63

Ostriker, J.P., & McKee, C.F. 1988, Rev. Mod. Phys. 60, 1

Ostriker, J.P., & Silk, J. 1973, ApJ, 184, L113

Paciesas, W.S., et al. 1999, ApJS, 122, 465

Paczynski, B. 1998, in Gamma-Ray Bursts: 4th Huntsville Symposium, eds. C.A. Meegan, R.D. Preece and T.M. Koshut (Woodbury New York: American Institute of Physics), p783

Paczynski, B. 2001, in Supernovae and gamma-ray bursts: the greatest explosions since the Big Bang, eds. M. Livio, N. Panagia and K. Sahu (Cambridge University Press: Cambridge), p1

Padoan, P., Jimenez, R., & Jones, B. 1997, MNRAS, 285, 711

Palla, F., Salpeter, E.E., & Stahler, S.W. 1983, ApJ, 271, 632

Panaitescu, A., Kumar, P., & Narayan, R. 2001, ApJ, 561, L171

Partridge, R.B. 1974, ApJ, 192, 241

Peebles, P.J.E. 1969, ApJ, 155, 393

Peebles, P.J.E. 1993, Principles of Physical Cosmology (Princeton: Princeton University Press)

Peebles, P.J.E., & Dicke, R.H. 1968, ApJ, 154, 891

Press, W.H., & Schechter, P. 1974, ApJ, 187, 425

Qian, Y.-Z., Sargent, W.L.W., & Wasserburg, G.J. 2002, ApJ, 569, L61

Qian, Y.-Z., & Wasserburg, G.J. 2001, ApJ, 549, 337

Qian, Y.-Z., & Wasserburg, G.J. 2002, ApJ, 567, 515

Rakavy, G., Shaviv, G., & Zinamon, Z. 1967, ApJ, 150, 151

Razoumov, A.O., & Scott, D. 1999, MNRAS, 309, 287

Rees, M.J. 1984, ARAA, 22, 471

Rees, M.J. 1990, Science, 247, 817

Rees, M.J., & Meszaros, P. 1992, MNRAS, 258, 41p

Ricotti, M., Gnedin, N.Y., & Shull, J.M. 2001, 560, 580

Rossi, S., Beers, T.C., & Sneden, C. 1999, in The Third Stromlo Symposium: The Galactic Halo, eds. B.K. Gibson, T.S. Axelrod,and M.E. Putman, p265

Ryan, S.G., Norris, J.E., & Beers, T.C. 1996, ApJ, 471, 254

Salpeter, E.E. 1955, ApJ, 121, 161

Saslaw, W.C., & Zipoy, D. 1967, Nature, 216, 976

Schaerer, D. 2002, A& A, 382, 28

Schwarzschild, M., & Spitzer, L. 1953, Observatory, 73, 77

Sedov, L.I. 1959, Similarity and Dimensional Methods in Mechanics (New York: Academic Press)

Shapiro, P.R., & Kang, H. 1987, ApJ, 318, 32

Shapiro, P.R., Raga, A.C., & Mellema, G. 1997, Structure and Evolution of the Intergalactic Medium from QSO Absorption Line Systems (Proceedings of the 13th IAP Astrophysics Colloquium), eds. P. Petitjean and S. Charlot, pp. 41 -45

Shull, J.M., et al. 1980, AJ, 237, 769

Shull, J.M., et al. 1999, AJ, 118, 1450

Shchekinov, Y.A., & Edelman, M.A. 1978, Sov. Astro. Lett., 4, 234

Shklovsky, I.S. 1960, "Cosmic Radio Waves" (Harvard University Press: Cambridge)

Shklovsky, I.S. 1968, Supernovae (New York: Interscience Publishers)

Silk, J. 1977, ApJ, 211, 638

Stahler, S.W. 1986, PASP, 98, 1081

Stecher, T.P., & Williams, D.A. 1967, ApJ, 149, L29

Steidel, C.C., Giavalisco, M., Pettini, M., Dickinson, M., & Adelberger, K.L. 1996, ApJ, 462, L17

Steinmetz, M., & Bartelmann, M. 1995, MNRAS, 272, 570

Stockman, H.S., & Mather, J.C. 2000, Imaging the Universe in Three Dimensions: Proceedings from ASP Conference Vol. 195, eds. W. van Breugel and J. Bland-Hawthorn, p 415

Subramanian, K., Cen, R., & Ostriker, J.P. 2000, ApJ, 538, 528

Sutherland, R.S., & Dopita, M.A. 1993, ApJS, 88, 253

Syer, D., & White, S.D.M. 1996, astro-ph/9611065

Takeda, H., Sato, H., & Matsuda, T. 1969, Prog. Th. Phys., 41, 840

Tarbet, P.W., & Rowan-Robinson, M. 1982, Nature, 298, 711

Taylor, G.I. 1950, Proc. Roy. Soc. London, A, 101, 159

Tegmark, M., Silk, J., Rees, M.J., Blanchard, A., Abel, T., & Palla, F. 1997, ApJ, 474, 1

Terlevich, R., Tenorio-Tagle, G., Franco, J., & Melnick, J. 1992, MNRAS, 255, 713

Tielens, A.G.G.M., Seab, C.G., Hollenbach, D.J., & McKee, C.F. 1987, 319, L109

Tohline, J.E. 1980, ApJ, 239, 417

Tremaine, S., et al. 2002, ApJ, 574, 740

Tumlinson, J., & Shull, J.M. 2000, ApJ, 528, L65

Turner, E.L. 1980, ApJ, 242, L135

Turner, E.L., Ostriker, J.P., & Gott, J.R. III 1984, ApJ, 284, 1

Tyson, J.A. 1983, ApJ, 272, L135

Ueda, H., Shimasaku, K., Suginohara, T., & Suto, Y. 1994, PASJ, 46, 319

Valageas, P., & Silk, J. 1999, A& A, 347, 1

Vishniac, E. 1983, ApJ, 274, 152

Wallerstein, G. 1984, ApJ, 278, 663

Wasserburg, G.J., & Qian, Y.-Z. 2000, ApJ, 529, L21

Weinberg, S. 1972, "Gravitation and Cosmology" (New York: John Wiley & Sons), p453

Wheeler, J.C., Mazurak, T.J., & Sivaramakrishnan, A. 1980, ApJ, 237, 781

Wheeler, J.C., Yi, I., Hoeflich, P., & Wang, L. 2000, ApJ, 537, 810

White, S.D.M. 1984, ApJ, 286, 38

Woosley, S.E. 1986, in Nucleosynthesis and Chemical Evolution, ed. B. Hauck, A. Maeder and G. Meynet (Switzerland: Geneva Obs), p1

Woosley, S.E., & Weaver, T.A. 1982, in Supernovae, eds. M.J. Rees and R.J. Stoneham (Dordrecht: Reidel), p79

Woosley, S.E., & Weaver, T.A. 1995, ApJS, 101, 181

Yoneyama, T. 1972, PASP, 24, 87

Yoshii, Y., & Sabano, Y. 1979, PASJ, 31, 505

Yoshii, Y., & Saio, H. 1986, ApJ, 301, 587

A. Magnification of Pop III Sources by Gravitational Lensing

We determine the fraction of area in the background source plane at redshift z_S, that is magnified by a factor of $\geq \mu$ by foreground objects, primarily clusters of galaxies. The magnification regime in which we are interested is $\mu \geq 10$. We will first derive a general relationship between the magnification (μ) and source plane coordinate (x): $\mu \propto 1/x$ for any singular density profile. Then, we will use the singular isothermal sphere thanks to its ease of analytic treatment, which has the same $\mu \propto 1/x$ relation, to model clusters of galaxies

AAS LaTeX macros v5.0.

to compute the gravitational lensing cross section at the high μ end. The computed lensing cross section is cross-checked by observations to ensure consistency.

We express the magnification μ as a function of x, the source plane proper coordinate (Fig 13). It is well known that $\mu \approx 1/x$ in the small x, high μ limit, for both a point mass lens (Vietri & Ostriker 1983) and a singular isothermal sphere lens (SIS; Turner, Ostriker & Gott 1984). For simplicity we will consider only axisymmetric lenses. We will generalize this property of μ in the small x, high μ limit to any lens system as long as the lensing bending angle, θ, as a function of proper impact parameter, b, does not increase as fast as b. It is noted that $\theta \propto b$ for a uniform mass sheet, $\theta =$ constant for a SIS, and $\theta \propto 1/b$ for a point mass. From Figure 10 we can readily write down the lens equation as:

$$\alpha + \beta = \frac{b}{D_L}, \quad \beta = \frac{x}{D_S}, \quad \alpha D_S = \theta D_{LS}. \tag{A1}$$

The above equation relates the angular position of the image, $\alpha + \beta$, to the position of the source, β (both with respect to some reference direction) through the bending angle, θ. D_S, D_L and D_{LS} are the angular diameter distance between the observer and the source, between the observer and the lens, and between the lens and the source, respectively. b is the proper impact parameter relative to the lens center. Expressing the bending angle θ as $\theta \equiv \theta_0(b/b_0)^m$ $(m < 1)$, we can rewrite the above lens equation as:

$$\theta_0(b/b_0)^m = bD_S/(D_L D_{LS}) - x/D_{LS}. \tag{A2}$$

In the limit $x \to 0$, the solution for the impact parameter is $b = b_0[b_0 D_S/(\theta_0 D_L D_{LS})]^{1/(m-1)}$ (Einstein radius), and $dx/db = (1-m)D_S/D_L$. It is noted that the requirement $m < 1$ is to guarantee a solution, i.e., the existence of an Einstein radius. Then, it is straightforward to show that, at small x limit, the magnification is

$$\mu(x) = \frac{b}{x}\frac{db}{dx}(\frac{D_S}{D_L})^2 = \frac{K}{x} \tag{A3}$$

with the constant K, independent of x, being

$$K = (\frac{b_0 D_S}{\theta_0 D_L D_{LS}})^{1/(m-1)} \frac{D_S}{D_L}\frac{b_0}{1-m}. \tag{A4}$$

We note that, for any (centrally) singular density profile, m is less than unity. It has been shown by Syer & White (1996) and Subramanian, Cen, & Ostriker (2000) that the density profile in the inner regions of dark matter halos, which are formed through hierarchical gravitational clustering/merging in the conventional Gaussian structure formation models, is $\rho(r) \propto r^{-3(3+n)/(5+n)}$, where n is the linear power spectrum index at the relevant scales. For the scales of interest, we have $n \sim -2$ to -1 for cold dark matter models, giving $\rho(r) \propto r^{-1.5}$

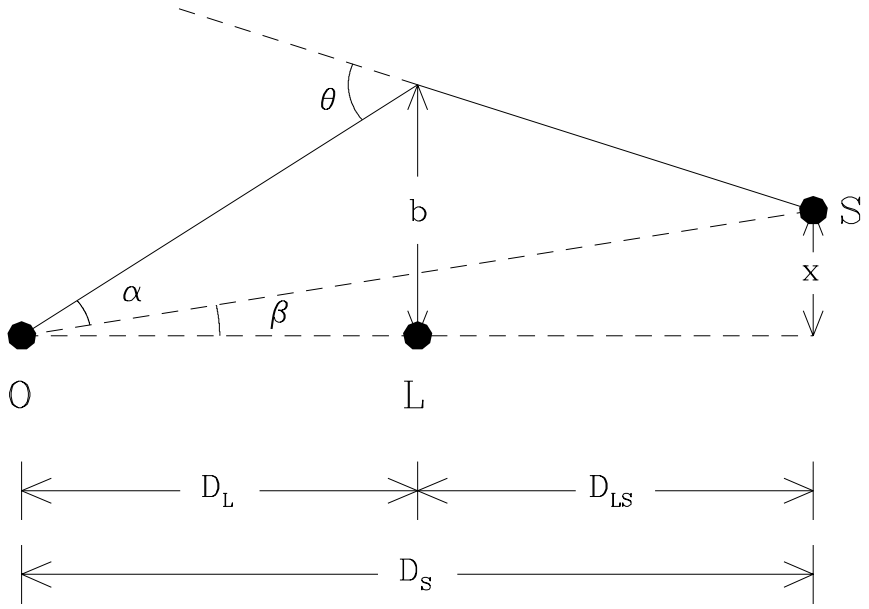

Fig. 13.— shows the gravitational lensing optics. O, L and S are the observer, the lens and the source, respectively. D_L, D_S and D_{LS} are angular diameter distance from observer to the lens, from observer to the source, and from the lens to the source, respectively. b and x are the impact distance and source plane coordinate, respectively. θ is the light bending angle when passing by the lens at impact distance b.

to $\rho(r) \propto r^{-1.0}$. These inner slopes of halos were borne out in N-body simulations (Navarro, Frenk, & White 1997; Moore et al. 1999). Thus, we should expect $\mu \propto 1/x$ at small x for halos formed in hierarchical structure formation models, including those of galaxy cluster size. Moreover, cooling and subsequent condensation of baryons in the centers of halos may further steepen the density profiles in the inner regions.

Having deduced the universal $\mu \propto 1/x$ relation at the small x end, we will now carry out further calculations by adopting the SIS model, because of its analytical simplicity and because of its astrophysical relevance as shown in many statistical studies (Gott & Gunn 1974; Tyson 1983; Turner et al. 1984; Hinshaw & Krauss 1987; Narayan & White 1988; Wu 1989; Fukugita & Turner 1991; Mao 1991). This is further justified if μ is normalized at a somewhat lower value, where some data from current observations exist. We note that, for individual multiply imaged observed quasars, it is clear that one needs to include ellipticities of the lenses for realistic modeling. For example, one cannot produce quadruples with an axisymmetric lens (Narayan & Grossman 1989; Blandford et al. 1989). However, for our purpose of calculating the magnification cross section at moderate-to-high range $\mu \sim 10 - 100$, the assumption of axisymmetry of lenses should be adequate. For a SIS the bending angle, θ_0, conveniently independent of impact parameter, is (Turner et al. 1984)

$$\theta_0 = 4\pi(\frac{\sigma_{||}}{c})^2, \tag{A5}$$

where c is the speed of light and $\sigma_{||}$ is the line of sight velocity dispersion of the SIS lens. With equation (A5) we can solve equation (A2) with the following solution at the $x \to 0$ limit: $b = \frac{\theta_0 D_L D_{LS}}{D_S}$ and $\frac{db}{dx} = \frac{D_L}{D_S}$. Inserting this solution into equation (A3) yields the small x limit of the $x - \mu$ relation for a SIS lens:

$$x(\mu) = \frac{4\pi}{\mu}(\frac{\sigma_{||}}{c})^2 D_{LS}. \tag{A6}$$

A SIS would subtend a solid angle in the source plane $\Delta\Omega$ within which the luminosity of a source is magnified by $\geq \mu$: $\Delta\Omega = \frac{\pi x^2(\mu)}{D_S^2}$. Thus, the total probability of a *random* source at z_S of being magnified by $\geq \mu$ can be obtained by adding up all the foreground lenses. This is done by integrating $\Delta\Omega/4\pi$ over lenses of all masses and over all redshifts up to the source redshift, z_S, resulting in a double integral:

$$P_{random} = \int_0^\infty \int_0^{z_S} \frac{\pi x^2}{4\pi D_S^2} n(M_A, z) 4\pi r^2 \frac{dr}{dz} dz dM, \tag{A7}$$

where $n(M_A, z)$ is the mass function of halos at redshift z. To make the subsequent calculation more analytically tractable, we assume

$$n(M_A, z) = (1+z)^{-w} g(M_A), \tag{A8}$$

where

$$g(M_A) = (4 \times 10^{-5}/M_*)(M_A/M_*)^{-1} \left[1 + (M_A/M_*)^{-1}\right] \exp(-M_A/M_*)\ h^3\mathrm{Mpc}^{-3} \qquad \text{(A9)}$$

is the differential cluster mass function at $z = 0$, taken from Bahcall & Cen (1993). M_A is the observed cluster mass within the Abell radius ($r_A = 1.5h^{-1}$Mpc) and $M_* = 1.8\times10^{14}\ h^{-1}\mathrm{M}_\odot$. The term $(1+z)^{-w}$ is intended to approximately describe the evolution of the overall cluster mass function with redshift. The cluster mass, M_A, defined within the Abell radius, r_A, may be related to $\sigma_{||}$ for the SIS model by

$$\sigma_{||}^2 = \frac{GM_A}{2r_A}, \qquad \text{(A10)}$$

where G is the gravitational constant. Combining equations (A6) and (A10) indicates that $x^2 \propto M_A^2$. It is instructive to examine the behavior of the following term, $x^2 g(M_A)$, which contains all the dependence of the integrand of the integral in equation (A7) on M_A. Since $x^2 g(M_A)$ is constant at the low M_A end and $x^2 g(M_A) \propto (M_A/M_*)\exp(-M_A/M_*)$ at the high M_A end, the integral over M_A in equation (A7) is convergent on both ends and dominated by massive clusters near the exponential downturn at about $M \sim 1 \times 10^{15} M_\odot$. Consequently, for our purpose, we need only to be accurate on the high mass end near the exponential downturn for $g(M_A)$ and its redshift distribution characterized by parameter w. Substituting equations (A6, A8, A9, A10) into equation (A7) [and making use of the simple relations in an $\Omega_0 = 1$ universe: $D_L = R_H(1 - 1/\sqrt{1+z_L})$, $D_S = R_H(1 - 1/\sqrt{1+z_S})$, $D_{LS} = R_H(1/\sqrt{1+z_L} - 1/\sqrt{1+z_S})$ and $\frac{dr(z)}{dz} = \frac{1}{2}R_H(1+z)^{-3/2}$] yields

$$\begin{aligned} P_{random} &= \frac{2B\pi^3 G^2 R_H^3}{c^4 r_A^2 \mu^2}\left(1 - \frac{1}{\sqrt{1+z_S}}\right)^{-2} \int_0^\infty M_A^2 g(M_A) dM \\ &\quad \times \int_0^{z_S} \left(1 - \frac{1}{\sqrt{1+z}}\right)^2 \left(\frac{1}{\sqrt{1+z}} - \frac{1}{\sqrt{1+z_S}}\right)^2 (1+z)^{-3/2-w} dz \\ &= \frac{1.0 \times 10^{-5} B\pi^3 G^2 R_H^3 M_*^2}{c^4 r_A^2 \mu^2}\left(1 - \frac{1}{\sqrt{1+z_S}}\right)^{-2} \int_0^\infty t(1+t^{-1})\exp(-t) dt \\ &\quad \times \int_0^{z_S} \left(1 - \frac{1}{\sqrt{1+z}}\right)^2 \left(\frac{1}{\sqrt{1+z}} - \frac{1}{\sqrt{1+z_S}}\right)^2 (1+z)^{-3/2-w} dz. \end{aligned} \qquad \text{(A11)}$$

All constants in equation (A11) are in c.g.s. units, except R_H, which is in Mpc. Note that we have also inserted a constant B in equation (A11), which serves to absorb the uncertainties due to other factors which either cannot be accurately treated here or are unknown, including background cosmology, deviations of density profiles from singular isothermal spheres, gravitational lensing due to other astronomical objects and uncertainties in the observed cluster mass function. The normalization of B will be set by comparing to observations at

$\mu > 2$. Now expanding all the constants and integrating equation (A11) with respect to t ($\equiv M_A/M_*$), we obtain

$$P_{random} = \frac{0.036B}{\mu^2}(1 - \frac{1}{\sqrt{1+z_S}})^{-2} I(z_S, w), \tag{A12}$$

where $I(z_S, w) \equiv \int_0^{z_S}(1 - \frac{1}{\sqrt{1+z}})^2(\frac{1}{\sqrt{1+z}} - \frac{1}{\sqrt{1+z_S}})^2(1+z)^{-3/2-w}dz$. The integral $I(z_S, w)$ can be done analytically (but the resultant expression is quite lengthy) and here we just give the final numbers for specific z_S and w. For $z_S = 17.0$, $P_{random} = (1.1 \times 10^{-3}, 6.8 \times 10^{-4}, 4.2 \times 10^{-4}, 2.1 \times 10^{-4})B/\mu^2$, for $w = (0.0, 0.5, 1.0, 2.0)$, respectively. It shows that P_{random} only weakly depends on w, because the integral is dominated by the moderate redshift range $z \sim 0.5 - 1.0$.

It is justified to only consider the large splitting events since the lensing cross section is dominated by massive clusters which give rise to large splittings ($> 1''$). For the sake of concreteness we will adopt $w = 0.5$, which is consistent with the relatively wild evolution of cluster density up to redshift about unity (e.g., Bahcall, Fan, & Cen 1997). As we will show below, the final results (P_{clust}) turn out to be extremely weakly dependent on w. Furthermore, we take $B = 3.4$ to normalize P_{random}:

$$P_{random}(\mu) = \frac{2.0 \times 10^{-3}}{\mu^2}, \tag{A13}$$

which gives $P_{random}(\mu = 2) = 4.0 \times 10^{-4}$. Since we are integrating the observed clusters to obtain the lensing probability and the same clusters are also responsible for observed gravitational lensing events, we can make a consistency check. For the Hewitt & Burbidge (1989) quasar catalog of 4250 quasars there are two confirmed multiple image lens systems with splitting $> 1''$, which corresponds to multiple lensing probability of $4.7 \times 10^{-4} (= 2/4250)$, i.e., $P = 4.7 \times 10^{-4}$ for $\mu > 2$ (in the singular isothermal sphere case). Thus, our adopted normalization is consistent with the observed value of $P = 4.7 \times 10^{-4}$ for $\mu > 2$. Considering possible selection biases (Turner 1980; Cen et al. 1994a; Kochanek 1995) and the countervailing effect that the observed quasar sample is at significantly lower redshift than $z = 17$ considered here, we argue that the adopted normalization is reasonable. From this we see that a *random* source at $z_S = 17$ has a rather small probability of $\leq 10^{-3}$ being very strongly lensed.

We will now examine the case where we do not sample the sky randomly, rather observe a set of selected regions centered on massive clusters. The cross section for magnification $\geq \mu$ in the source plane is $\pi x^2(\mu)$, so the solid angle within which the sources will be magnified by $\geq \mu$ is $\pi x^2(\mu)/D_s^2$. Integrating $\pi x^2(\mu)/D_s^2$ over a pre-selected set of clusters with mass $M_A \geq M_{lim}$ in the redshift range $z = z_1$ to z_2 and dividing the integral by the number of

clusters pre-selected gives the mean solid angle for source magnification $\geq \mu$.

$$\langle \Omega(>\mu) \rangle = \frac{\int_{M_{lim}}^{\infty} B' g(M_A) dM \int_{z_1}^{z_2} \frac{\pi x^2}{D_S^2} (1+z)^{-w} 4\pi r^2 \frac{dr}{dz} dz}{N_{cl}(z_1, z_2, M_{lim})}, \tag{A14}$$

where $N_{cl}(z_1, z_2, M_{lim}) \equiv \int_{M_{lim}}^{\infty} g(M_A) dM \int_{z_1}^{z_2} (1+z)^{-w} 4\pi r^2 \frac{dr}{dz} dz$ is the total number of clusters selected (a normalization factor). Dividing the mean solid angle for source magnification $\geq \mu$ by the field of view yields the mean probability of *a source* in such selected fields which will be magnified by $\geq \mu$:

$$P_{clust}(\mu) = \frac{\langle \Omega(>\mu) \rangle}{\Omega_{FOV}}, \tag{A15}$$

where Ω_{FOV} is a telescope's field of view. As an example, let us take $M_{lim} = 1 \times 10^{15} M_{\odot}$, $z_1 = 0.0$ and $z_2 = 0.4$, which yields $N_{cl}(0.0, 0.4, 1 \times 10^{15}) = (3020, 2669, 2362, 1852)$, for $w = (0.0, 0.5, 1.0, 2.0)$, respectively, in an $\Omega_0 = 1$, $H = 50$km/s/Mpc universe. Similar to equation (A11), we can integrate equation (A14) for $z_S = 6.0$, $z_1 = 0.0$, $z_2 = 0.4$ and $M_{lim} = 1.0 \times 10^{15} M_{\odot}$ and the result is: $P_{clust}(\mu) = (6.7 \times 10^{-2}, 6.7 \times 10^{-2}, 6.8 \times 10^{-2}, 6.9 \times 10^{-2}) \frac{1}{\mu^2} (\frac{\Omega_{FOV}}{25 \text{ arcmin}^2})^{-1}$. Although an adjustment parameter B' in equation (A14), which is different from B in equation (A11) to reflect the fact that the uncertainties involved are somewhat different (for example, since the probability is normalized per cluster, the uncertainty in the amplitude of the observed cluster mass function cancels out), for clarity and simplicity we adopt $B' = B = 3.3$. The result indicates that $P_{clust}(\mu)$ is nearly independent of w, unlike P_{random}, which depends on w, giving

$$P_{clust}(\mu) = \frac{6.7 \times 10^{-2}}{\mu^2} \left(\frac{\Omega_{FOV}}{25 \text{ arcmin}^2} \right)^{-1}. \tag{A16}$$

Comparing P_{clust} with P_{random}, for the case with $w = 0.5$, for example, we see that one gains a factor of 34 in the cluster centered survey compared to a random survey, for a field of view of $\Omega_{FOV} = 25$ arcmin^2. The relative gain decreases with increasing size of the field of view, and the two probabilities become equal at $\Omega_{FOV} = 838$ arcmin^2, above which the calculation of P_{clust} is no longer valid due to multiple clusters in a single field. Note that, although the mean probability of a source within the field of view is inversely proportional to Ω_{FOV}, the total number of magnified sources per field of view is $P_{clust} \Omega_{FOV} \Sigma_{src}$ (where Σ_{src} is the surface density of source *src*, which is either *gal* or *SN* in this study), which is independent of Ω_{FOV}. The physical reason for having a relative increase in the probability of magnified sources is that the clusters of galaxies are rare targets and hence a *random* field of view has a small probability of intersecting a cluster. We note that P_{random} is still valid even in the case of multiple clusters in a single field. However, the calculation of P_{random} breaks down when multiple clusters are *precisely* aligned along the line of sight. But such cases are likely to be negligibly few. We further note that the spatial clustering of galaxy clusters would further boost the gain of P_{clust} over P_{random}, but we will not consider this effect here.